Intake Air Dynamics on a Turbocharged SI-Engine with Wastegate

Per Andersson

Intake Air Dynamics on a Turbocharged SI-Engine with Wastegate

peran@isy.liu.se
http://www.fs.isy.liu.se
Department of Electrical Engineering,
Linköping University,
SE–581 83 Linköping,
Sweden.

To Ulrika

Abstract

On turbocharged spark-ignited (SI) engines with wastegate the position of the wastegate changes the exhaust manifold pressure. A secondary effect of this is that the residual gas mass trapped inside the cylinder at exhaust valve closing changes and causes the volumetric efficiency to change. The volumetric efficiency is used to estimate air-mass-to-cylinder which is important for good air/fuel ratio control.

Air-mass to-cylinder is not directly measurable so observers for air-mass flow to the cylinder are therefore often proposed. For observers with one state for intake manifold pressure and proportional feed-back from measured state, there is a tradeoff whether to estimate intake manifold pressure or air-mass-to-cylinder. A new nonlinear air-mass-to-cylinder observer is suggested with two states: one for intake manifold pressure and one for the in-cylinder air-mass offset compared to expected using the volumetric efficiency.

The exhaust manifold pressure can change rapidly in an engine with wastegate. A method to estimate the exhaust manifold pressure is presented for diagnosis of wastegate and turbocharger on SI-engines. It does not use any extra sensors in the exhaust system after the calibration. The exhaust manifold pressure estimator is validated using a series of wastegate steps. The exhaust pressure estimation is designed for steady-state conditions and the validation shows that it works well and converges within 1 to 4 seconds.

Finally a method to detect leakages in the exhaust manifold is suggested. Leakage detection before the three way catalyst is important since untreated emissions leak out and since, due to standing waves in the exhaust system, air can leak in and disturb the air/fuel ratio controller. To extend the operating region for the detection, the proposed method utilizes both information on leaks out of the manifold and information on presence of oxygen in the exhaust manifold.

ii

Acknowledgments

This work has been performed under Professor Lars Nielsen at Vehicular Systems, Dept. of Electrical Engineering, Linköping University, Sweden and I am grateful to him for letting me join this excellent group of people and for the support provided during this work. I would also like to thank the staff at Vehicular Systems for creating such a positive atmosphere.

Marcus Klein and Ylva Nilsson are also acknowledged for proofreading early versions of the manuscript and for the research discussions we had. I would also like to thank Dr. Erik Frisk for interesting discussions and his help with LATEX and Emacs. For their support during the project, SAAB AUTOMOBILE AB and MECEL AB are acknowledged. Finally my supervisor Dr. Lars Eriksson is greatly acknowledged for his patience and encouragement.

This work has been supported by the Swedish Agency for Innovation Systems (VINNOVA) through the center of excellence ISIS (Information Systems for Industrial Control and Supervision).

Linköping, January 2002

Per Andersson

CONTENTS

1

INTRODUCTION

Today turbocharged spark-ignited (SI) engines are getting more popular as they provide good fuel economy and high power output. On most of these engines there is a device called wastegate (Watson and Janota, 1982; Heisler, 1997), which is located in the turbocharger, on the exhaust side, with the purpose to control the power to the turbine. When the wastegate is opened the power drops and vice versa, and often this device is controlled by a pneumatic actuator which is coupled to the boost pressure after the compressor. The valve setting of the wastegate or the actuator is not normally measured. Few sensors are located on the exhaust side of the engine; usually there are only oxygen sensors. On the other hand, on most engines there are more sensors in the intake system. Here, the information that is the result of a change in wastegate setting is studied using the available sensors in the intake system. An experiment to open the wastegate at constant speed and load is made to give some indications of what kind of information that is present in the intake system when the wastegate is moved. During the experiment the air-mass flow is governed by a controller whose objective is to maintain constant air-mass flow. The result of the experiment is shown in Figure 1.1, where the exhaust manifold pressure drops when the wastegate is opened. What is interesting is that the intake manifold pressure also drops when the exhaust pressure drops. Thus, information about exhaust manifold conditions is present in the intake system.

One especially interesting quantity in engines is the air-mass flow to the cylinders. Knowledge of it is important when deciding how much fuel to inject. Air-mass flow to the cylinders is not measurable so it has to be estimated. In Chapter 2 two common principles for air-mass estimation are described and a
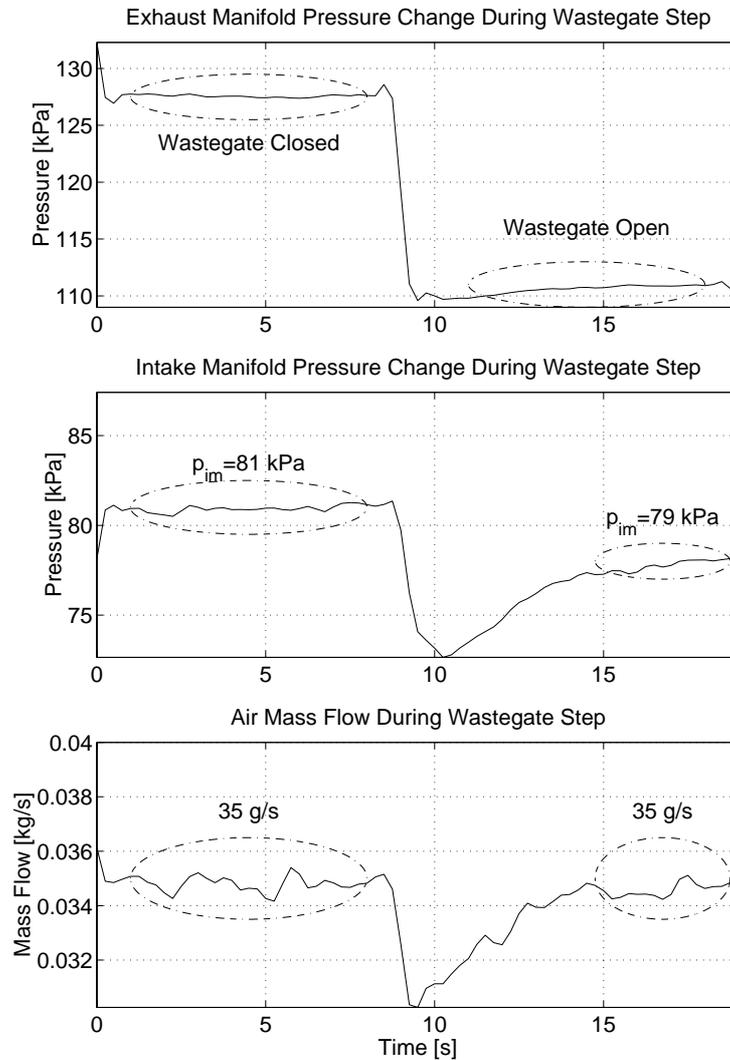
Figure 1.1: The engine is run at a constant speed of 2500 RPM and at a constant load (air-mass flow). *Top:* When the wastegate is opened at 8 seconds, the exhaust pressure drops. *Center:* In the intake manifold there is a pressure drop of 2 kPa when the wastegate is opened. *Bottom:* The air-mass flow is constant except for a transient when the wastegate is changing position.

background on air/fuel ratio control is given. In Chapter 4 two speed-density methods are compared for air-mass flow to cylinder estimation and then a new model for air-mass-to-cylinder is proposed together with an observer for this model. This observer features an additional state that describes changes in in-cylinder air-mass compared to what is expected through the volumetric efficiency map.

In Figure 1.1 the intake manifold pressure drops when the wastegate is opened. The observer suggested, in Chapter 4, gives useful information of whether the cylinder is filled with expected air-mass or not. If it is not, the change is assumed to be caused by a change in exhaust manifold pressure. A model-based estimator for the exhaust manifold pressure that utilize this information is proposed in Chapter 5. It uses only information from the intake side, meaning that no additional sensors are needed after calibration. The estimator is validated using step changes in wastegate position.

Finally in Chapter 6 exhaust manifold leaks before the first oxygen sensor is studied and the possibility to detect leakages without introducing additional sensors is investigated. When a leak is present emissions may either leak out or air leak into the exhaust manifold. When gases leak out there is a drop in exhaust manifold pressure which is supported by measurements. In the other case, where air leaks in, the additional oxygen that is supplied reaches the oxygen sensor and this can cause the engine to run rich. Measurements supports that the engine can run rich when there is a hole present in the exhaust manifold.

1.1 Contributions and Publications

1. A study of how common speed-density methods handle air-to-cylinder estimation during a wastegate step is made and a new observer for air-mass-to-cylinder is developed. This work was published at the SAE conference in Detroit 2001 (Andersson and Eriksson, 2001a). The air-mass-to-cylinder estimation problem for turbocharged SI-engines for various wastegate settings is illustrated. The contribution is an air-mass-to-cylinder observer that estimates the in-cylinder air-mass-offset.

2. An exhaust manifold pressure estimator for a turbocharged SI engine with wastegate is proposed. This application extracts information from the intake system about exhaust manifold conditions and does not require any additional sensors after calibration. It was published at the IFAC workshop Advances in Automotive Control in Karlsruhe 2001, (Andersson and Eriksson, 2001b). The contribution is a model based estimator for exhaust manifold pressure with few parameters.

3. Feasibility of a diagnosis method for exhaust manifold leakages before the first oxygen sensor is investigated. It utilizes information in the engine control system to detect leakages and does not need any additional sensors. This work is published at the SAE conference in Detroit 2002 (Andersson and Eriksson, 2002).

<div align="right">

2

</div>

<div align="right">

Background

</div>

There is an increasing demand for better fuel economy without sacrificing the power. One proposed concept to improve fuel economy and still have high power output is the down-sizing supercharging method which is studied in (Guzzella et al., 2000). Modern turbocharged SI-engines is commonly equipped with a by-pass valve called a wastegate. It by-passes some of the exhaust gases past the turbine and therefore reduces the available power to the turbine. Today the control of the wastegate is mapped or only used at high loads to reduce power to the turbine. In the future there is a possibility of additional fuel savings by active control of the wastegate also at part load, which is studied in (Eriksson et al., 2002). A side effect of controlling the wastegate is that the back pressure, that is the pressure in the exhaust manifold, varies with the valve setting of the wastegate. As the air-mass to cylinder varies with wastegate setting it is interesting to study common methods in their ability to estimate air-mass to cylinder for different settings of the wastegate.

2.1 Definition of Air/Fuel Ratio

Air/fuel ratio is the composition, on mass basis, of air and fuel in the cylinder when the intake valve has closed. Denote the mass of air by m_a and the mass of fuel by m_f. Then the air/fuel ratio is $\frac{m_a}{m_f}$. In most cases the normalized air/fuel ratio is used, that is the air/fuel ratio divided with the stoichiometric ratio. The stoichiometric air/fuel ratio $\left(\frac{A}{F}\right)_s$ describes the ratio of air and fuel, on mass basis, needed to fully combust the fuel. A typical stoichiometric reaction of air

and a fuel is shown below.

$$\underbrace{\underbrace{C_aH_bO_c}_{\text{Fuel}} + \underbrace{\left(a + \frac{b}{4} - \frac{c}{2}\right)(O_2 + 3.77N_2)}_{\text{Air}}}_{\text{Reactants}} \longrightarrow$$

$$\underbrace{aCO_2 + \frac{b}{2}H_2O + \left(a + \frac{b}{4} - \frac{c}{2}\right)3.77N_2}_{\text{Products}}$$
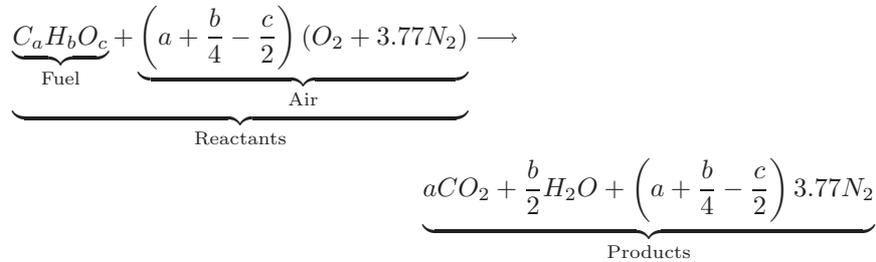
From this the stoichiometric air/fuel ratio is defined as

$$\left(\frac{A}{F}\right)_s = \frac{\left(a + \frac{b}{4} - \frac{c}{2}\right)\mathcal{M}_{air}}{\mathcal{M}_{fuel}} \approx \frac{\left(a + \frac{b}{4} - \frac{c}{2}\right)(32 + 3.77 \cdot 28)}{12a + b + 16c}$$

For isooctane C_8H_{18} this evaluates to $\left(\frac{A}{F}\right)_s \approx 15.1$ and for commercial gasoline the value of 14.7 is commonly used. In the following text the air/fuel ratio is used as a synonymous to the normalized air/fuel ratio λ

$$\lambda = \frac{m_a}{m_f \left(\frac{A}{F}\right)_s}$$

Two other common definitions is lean and rich mixture. In a lean mixture there is excess air, $\lambda > 1$, and in a rich mixture there is more fuel than the available air can oxidize, $\lambda < 1$. At stoichiometric conditions the normalized air/fuel ratio λ is one.

2.2   Air/Fuel Ratio Control

Air/fuel ratio control for spark ignited (SI) engines is a well studied topic over the years. Air/fuel control is necessary since the combustion in SI-engines is only possible for air/fuel ratios around stoichiometric. For slightly rich mixtures at the high temperatures and pressures inside the cylinder carbon monoxide is formed since there is not enough oxygen to fully oxidize the fuel to carbon dioxide. Rich mixtures can be used to maximize torque at full load. For lean mixtures, the efficiency on the other hand peaks, depending on lower pumping losses, lower heat transfer and higher ratio of specific heats for the mixture. This is another reason for air/fuel control since it provides a possibility of better fuel economy at part load by running the engine slightly lean. Good driveability is another issue especially during transients since the efficiency and torque development strongly depends on the air/fuel path. With bad air/fuel ratio control the engine torque fluctuates in a non-comfortable way.

There are also growing demands for lower emissions and this can partly be achieved with a three way catalyst. The TWC is most efficient for an air/fuel

ratio close to stoichiometric (Heywood, 1988; Degobert, 1995). This is currently the most important control problem as even small deviations from $\lambda = 1$ increase the emissions.

2.3 Two Common Air-Estimation Principles

For air/fuel ratio control the air-mass inducted into cylinder is important. The inducted air-mass depends on, among others, the pressure ratio between the exhaust manifold pressure and the intake manifold pressure (Heywood, 1988; Taylor, 1994). On SI engines the injected fuel mass is calculated based on the estimated mass of air in the cylinder. To maintain the stoichiometric air/fuel ratio, a change in exhaust manifold pressure will therefore require a change in injected fuel. Here two principles for estimating air-mass to cylinder is studied, namely the measured air-mass flow principle and the speed-density principle.

2.3.1 Measured Air-Mass Flow Principle

Injected fuel can be determined by measuring the air-mass flow into the engine and divide it by the air/fuel stoichiometric ratio. The air-mass flow sensor may typically be located far from the cylinders, close to the air filter. Consequently there is a large volume consisting of hoses, intercooler, and intake manifold separating the air-mass flow sensor from the cylinders. These are illustrated in Figure 2.1.
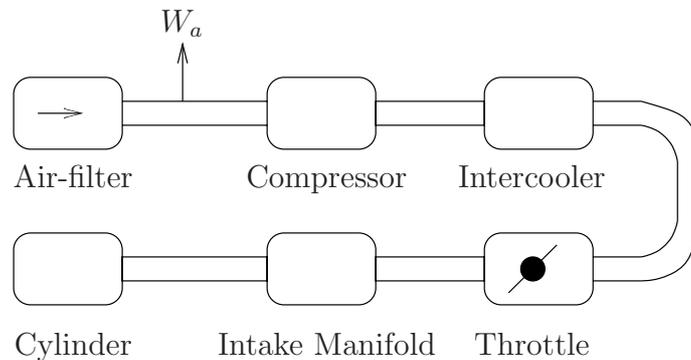
Figure 2.1: A simplified intake system to show the location of large air-volumes. There are volumes in the hoses between the sensor W_a, compressor, intercooler, and finally in the intake manifold. There is also a volume contribution from the intercooler.

Volumes introduce filling and emptying dynamics and a transient in the air-mass flow to the cylinders will therefore deviate from the measured air-mass

flow at the sensor. In Figure 2.2 this effect is shown as 5% transients in air-mass flow when the wastegate is operated during constant speed and air-mass flow of the engine. If the air-mass flow sensor is used to determine injected fuel there will therefore be an error of approximately 5% during the operation of the wastegate.

2.3.2 Speed-Density Principles

In the previous section the estimate of air-mass to cylinder is degraded by the dynamics caused by the volume between the air-mass flow sensor and the cylinder. Speed-density methods only use sensors in the intake manifold, together with volumetric efficiency to estimate air-mass flow to the cylinder. Thus they are independent of the dynamics between the air-mass flow sensor and the cylinder.

The speed-density methods uses volumetric efficiency, engine speed, and intake manifold pressure and temperature to determine the air-mass flow to cylinder, $W_c = \eta_{vol}(N, p_{im}) \frac{p_{im} V_d N}{R_{im} T_{im} n_r}$. A drawback of the speed-density methods is that the intake manifold pressure is subjected to noise. To reduce the intake manifold pressure noise, caused by engine pumping and standing waves, observers for mean intake manifold pressure have been proposed (Hendricks et al., 1992; Fekete et al., 1995).

Volumetric efficiency, η_{vol}, is a nonlinear function which has to be represented. A standard method to represent volumetric efficiency is by a two-dimensional map, and to compensate it for density variations in the intake manifold (Heywood, 1988).

$$\eta_{vol}(N, p_{im}) = \frac{W_a R_{im} T_{im} n_r}{p_{im} V_d N} \qquad (2.1)$$

The volumetric efficiency can also be represented by a polynomial in speed N and intake manifold pressure p_{im}

$$\eta_{vol} = a_0 + a_1 N + a_2 N^2 + a_3 p_{im} \qquad (2.2)$$

In Figure 2.3 the mapped volumetric efficiency and the estimated instantaneous is shown when the wastegate is opened and closed. Exhaust manifold pressure drops rapidly when the wastegate valve is opened and results in less residual gases in the cylinder. More air can then enter the cylinder which increases the volumetric efficiency. In the lower plot of Figure 2.3 a stationary increase in η_{vol} of 3% is present as the conditions stabilize at 14 and 37 seconds. Speed-density methods with fix maps must therefore rely on feed-back from the oxygen sensor to compensate for the change in η_{vol}. A limitation when feed-back is used is the transport delay until the mixture reaches the sensor.
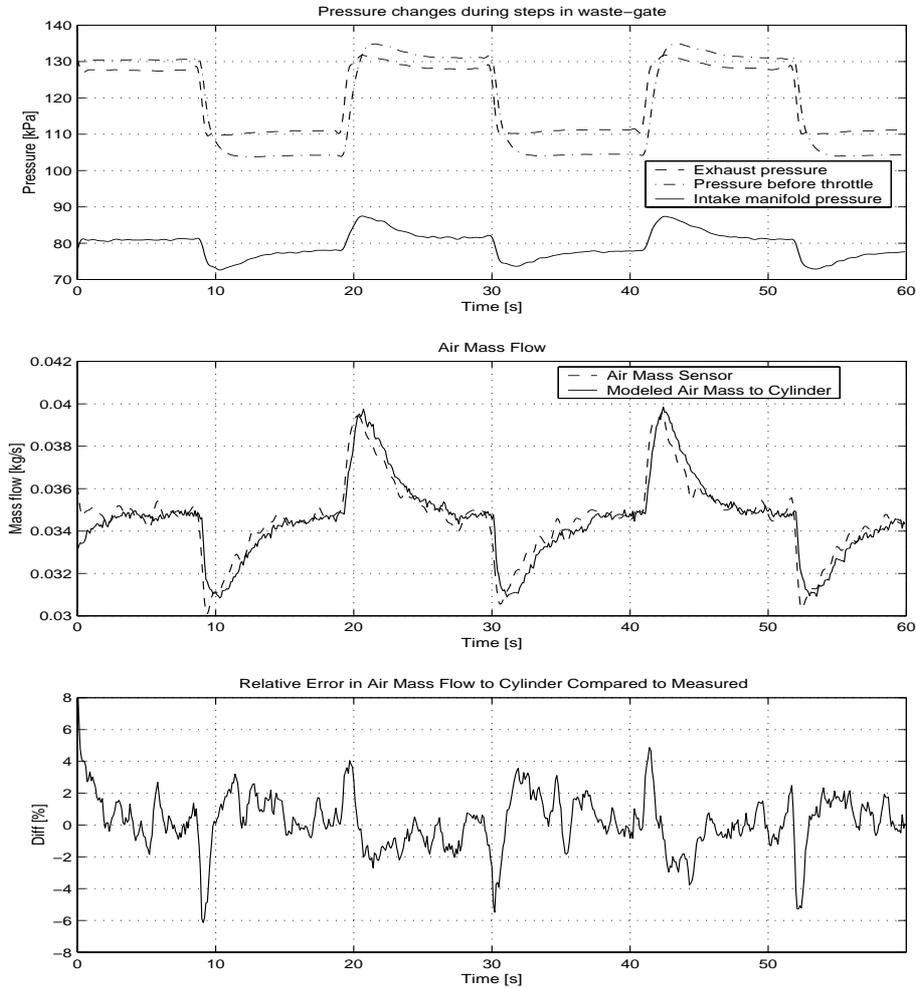
Figure 2.2: Comparison of measured air-mass and estimated air-mass to-cylinder using the suggested two-state observer in Chapter 4. *Top:* Pressure changes in exhaust system, intake system before throttle, and intake manifold pressure during manual operation of the wastegate. Wastegate is opened at 9, 30, and 52 seconds. It is closed at 19.5 and 41 seconds. During the test the engine speed and air-mass flow is held constant. *Center:* Measured air-mass flow, W_a, from the sensor and calculated air-mass flow to the cylinder $W_c = \eta_{vol}\left(N, p_{im}\right) \frac{p_{im} V_d N}{R_{im} T_{im} n_r}$. *Bottom:* The relative difference $100\left(\frac{W_c - W_a}{W_c}\right)$, is due to the filling and emptying dynamics of the intake system.
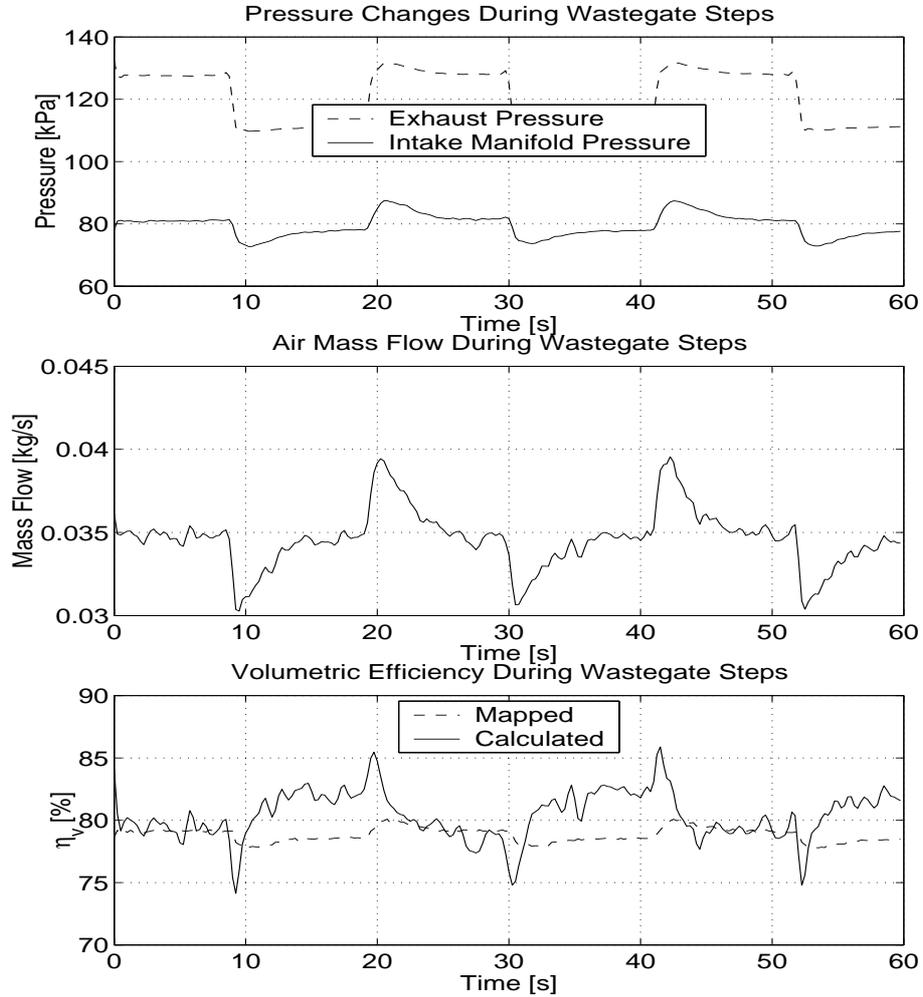
Figure 2.3: When the wastegate position have been changed the volumetric efficiency is influenced. *Top:* Pressure changes in exhaust system, intake system before throttle, and intake manifold pressure during manual operation of the wastegate. Wastegate is opened at 9, 30, and 52 seconds. It is closed at 19.5 and 41 seconds. During the test the engine speed is held constant. *Center:* Measured air-mass flow, W_a. As the wastegate is opened the air-mass flow decreases momentarily until the air-mass controller has opened the throttle more. The throttle controller tries to maintain a constant air-mass flow. *Bottom:* Calculated using Equation (2.1) and estimated volumetric efficiency using Equation (2.2) during the wastegate step.

<div align="right">

3

</div>

Experimental Setup

The research laboratory at Vehicular Systems consists of a control room and an engine test cell. A schematic of the experimental setup is shown in Figure 3.1. A turbocharged engine is used for experiments in this thesis. A research engine management system called Trionic 7 (T7) controls the engine. From the control room it is possible to monitor variables in T7, and also to change the value of some variables. There is also a separate measurement system connected to both production sensors and additional sensors on the engine.

3.1 Engine Test Cell

Here, a description is presented, of the engine and modifications made to it in order to make the measurements. Then the dynamometer and the control of it is described.

3.1.1 Engine and Sensors

The engine is a 2.3 dm^3 turbocharged SAAB 9^5 engine with wastegate. Compared to a production engine, this engine has additional holes drilled in the intake and exhaust system for the extra sensors. The usual pipe for short-circuiting the compressor at rapid throttle closings is not installed as SAAB did not recommend it when the engine is running in a test bench. Another modification to the engine is a handle to open the wastegate manually. For safety reasons the wastegate can not be forced to close with this device. The engine data is listed in Table 3.1.
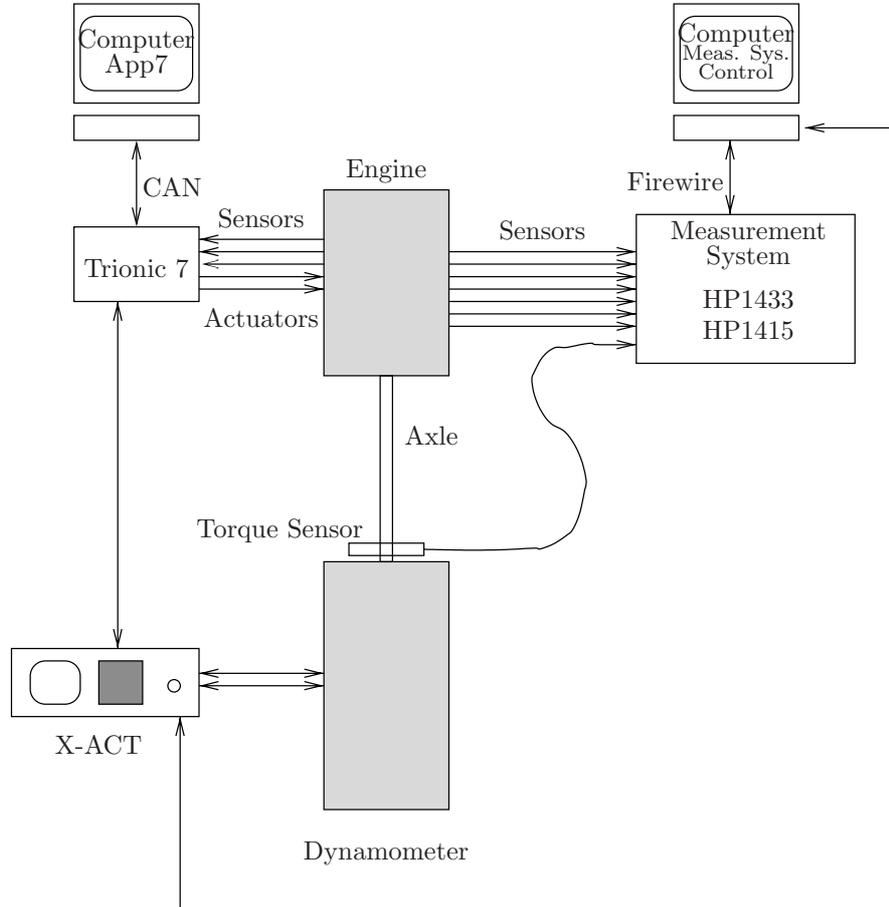
Figure 3.1: Experimental Setup. The two computers, measurement system and X-ACT are located in the control room. The engine, dynamometer and engine control system T7 are in the engine test cell.

Manufacturer	SAAB Automobile
Model	B235R
Displacement Volume	2.3 dm^3
Compression ratio	9.3
Maximum Power	170 kW @ 6200 RPM
Maximum torque	350 Nm @ 1900 RPM

Table 3.1: Engine Data

The additional pressure sensors and temperature sensors in the intake- and exhaust system are listed in Table 3.2 and their approximate locations are shown in the engine schematic in Figure 3.2. One wide band oxygen sensor is also fitted in front of the TWC in parallel to the discrete oxygen sensor.

Pressure between intercooler and throttle p_{ic}	Kistler Kristall 4293A2
Intake manifold pressure p_{im}	Kistler Kristall 4295A2
Exhaust manifold pressure p_{em}	Kistler Kristall 4295A5
Temperature between intercooler and throttle T_{ic}	Heraeus ECO-TS200s
Intake manifold temperature T_{im}	Heraeus ECO-TS200s

Table 3.2: Additional pressure and temperature sensors
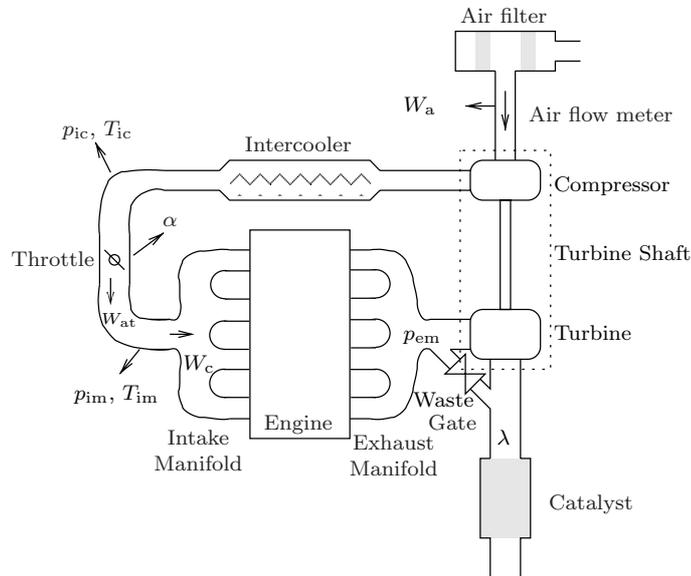
Figure 3.2: Engine Schematic with approximate sensor locations.

The production sensors that are used for measurements are: air-mass flow sensor, discrete oxygen sensor, and throttle plate angle. They are connected to the measurement instrument via a break-out-box placed at T7.

3.1.2   Dynamometer

An asynchronous Schenck Dynas$_2$ 220 dynamometer is fitted to the engine. With this type of dynamometer it is possible to both brake the engine and supply the engine with torque. The later is used to start the engine and gives the possibility to simulate downhill driving.

The dynamometer is controlled via a user interface called X-ACT. From X-ACT the engine speed and engine throttle position are controlled. It is also possible to control X-ACT from a computer via a serial interface (RS-232). This is done during engine mapping. The dynamometer data is listed in Table 3.3.

Manufacturer	Schenck
Model	$Dynas_2$ 220
Maximum power	220 kW
Maximum torque	450 Nm
Max speed	9500 RPM

Table 3.3: Dynamometer data

3.2 Control Room

Two computers are located in the control room. One controls the dynamometer and the measurement system. The other is connected to the engine control system T7 via a serial CAN-bus. The engine can be manually controlled from the control room using a computer with software from SAAB Automobile. The program is called App7 and it is an application development tool featuring possibilities to read and write parameters in T7. Here it is used to lock the throttle to a specific setting. App7 is mostly used to monitor engine parameters such as cooling water temperature, air/fuel ratio etc.

3.2.1 Measurements

All measurements are performed using a VXI-instrument, HP E1415A, from Hewlett-Packard. It can measure up to 64 channels with frequencies up to 2000 Hz and it features a built-in self calibration. The instrument can be customized by the signal conditioning modules that are chosen. The installed signal conditioning modules are listed in Table 3.4.

HP E1503A	Number of voltage channels	24
HP E1505	Number of current source channels	8
HP E1538A	Number of frequency, PWM channels	8

Table 3.4: Signal conditioning modules in HP E1415.

The current source module is used to measure temperature using PT200 elements, and the voltage over the element is measured. The air-mass sensor gives a frequency output and this is measured using the frequency unit. The fuel injection time is also measured using the this unit. The instrument is connected to a PC via a Firewire-bus. Two types of measurements are performed. First

an engine map is taken and then several experiments are performed where time signals are measured.

Engine Mapping

The engine mapping is performed using a program in HP-VEE, which is a special graphical programming language for test and automation. The program automated the mapping by controlling the engine speed and throttle position via the X-ACT together with the measurement system. The results are stored in a text file which is read into Matlab for processing. Engine mapping is performed with a sampling frequency of 10 Hz and the signals are low-pass filtered at 5 Hz to avoid aliasing. The engine mapping is performed from 1000 RPM up to 4800 RPM in steps of 250 RPM. The lower limit is due to severe vibrations at higher loads. In engine load, the mapping is performed in steps of approximately 15 Nm from closed throttle up to maximum torque in a total of 301 points. The engine is run 25 seconds in each work point before a 5 second sampling is started. For each work point the mean value of each sampled signal is stored except for air-mass flow where the median is stored instead. For the air-mass flow the median is used as the measured signal is subjected to short transients of high amplitude. The operating conditions that form the map is shown in Figure 3.3.
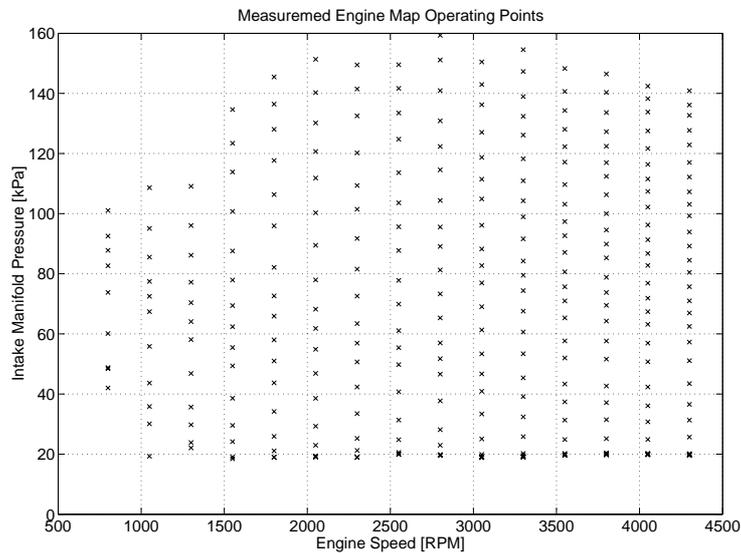
Figure 3.3: The visited engine operating points for the engine map. A total of 301 points are measured.

Dynamic Experiments

In the dynamic experiments, signals are monitored over time with a fix sampling frequency. The measurement instrument is controlled from Matlab using a program written in C as an interface and the measured data is directly available in Matlab for processing. The dynamic experiments are performed with three different objectives:

1. Measurement for studying how the intake side is influenced by changes in exhaust manifold pressure caused by an opening of the wastegate. To sample data during wastegate steps for the air-mass to-cylinder observer a sampling frequency of up to 1000 Hz is used. To reduce the time delay associated with alias filters they are disabled. The measured data is used in the air-mass to-cylinder observer in Chapter 4.

2. Measurements using steps in wastegate are made to study how information on the intake side can be used to estimate the exhaust manifold pressure in Chapter 5. The data collected for exhaust manifold pressure estimation is sampled using 10 Hz frequency since the stationary behavior is of highest interest.

3. Measurements for studying how leakages in the exhaust manifold influence exhaust manifold pressure and the air/fuel ratio of the engine. The research engine is equipped with additional oxygen sensor mountings, one for each cylinder on the exhaust manifold. On cylinder 3 this is used to replace the existing plug with a another plug with a drilled hole in it. These measurements are used in Chapter 6. A sampling frequency of 10 Hz is used here and the alias filters are set to 5 Hz

During the dynamic experiments an air-mass controller is active in T7, whose objective is to maintain constant air-mass flow. It succeeds in maintaining constant air-mass flow for intake manifold pressures below ambient.

Air-Mass-to-Cylinder Observer

The air-mass flow to the cylinder is not directly measurable and therefore several strategies to estimate it have been proposed (Hendricks et al., 1992; Chang et al., 1993; Shio and Moskwa, 1996; Tseng and Cheng, 1999; Kotwick et al., 1999; Jankovic and Magner, 1999). Most of the mentioned methods are developed with naturally aspirated engines in mind. The strategies to estimated air-mass flow combine the use of air-mass flow sensor, throttle plate angle as well as pressure and temperature sensors in the air intake system.

Two principles for air-mass estimation were described in Chapter 2, namely the measured air-mass flow principle and the speed-density principle. When air-mass-to-cylinder is estimated with these standard principles, it was illustrated that there is an error in estimated air-mass-to-cylinder when the wastegate is operated. For the measured air-mass flow, the transient when the wastegate position is changed only causes a short disturbance on the air/fuel ratio controller which is shown in Figure 2.2. When the wastegate is operated the volumetric efficiency changes and methods that rely on an accurate description of the volumetric efficiency (e.g. speed-density methods) will then estimate air-mass-to-cylinder inaccurately. As the estimated air-mass flow is used to calculate injected fuel mass there will be a small error in the air/fuel ratio. If the engine is equipped with feedback from an oxygen sensor this stationary error in air/fuel ratio will be detected and compensated for. Unfortunately there is a delay until the mixture is combusted and transported to the sensor and then the air/fuel controller needs time to converge to stoichiometric air/fuel ratio.

When air-mass-to-cylinder is estimated from measured air-mass flow there are filling and emptying dynamics in the intercooler, hoses, and intake manifold

that have to be accounted for. For speed-density methods only the intake manifold dynamics has to be accounted for. Therefore the speed-density method was chosen as the base of the air-mass-to-cylinder estimator. Another reason to use speed-density methods is that the pressure sensor is the fastest sensor in the intake manifold.

An observer for air-mass to-cylinder based on speed-density principle needs the mean intake manifold pressure, intake manifold temperature and the engine speed. The temperature varies slowly and therefore measurements are used. Measured intake manifold pressure is often filtered to reduce the noise from engine pumping and standing waves (Hendricks et al., 1992). A drawback of filtering the pressure signal is the time delay caused by the filter during transients. Observers are therefore often proposed since they can filter the signal and predict manifold pressure during transients. Here an analysis is made of a nonlinear observer using proportional feedback (Hendricks et al., 1992) and a nonlinear observer using pure integration (Tseng and Cheng, 1999). From the analysis a modified nonlinear observer is developed which takes advantage of the strengths of both structures and suits the conditions in a turbo charged spark ignition engine with wastegate. Especially the ability to estimate the same air-mass-to-cylinder as air-mass entering the manifold is studied for different settings of the wastegate. The strategy for estimating the air-mass flow to the cylinder thus relies on: a fast pressure sensor in the intake manifold p_{im}, measured intake manifold temperature T_{im} and pressure p_{ic} and temperature T_{ic} before the throttle, throttle plate angle α, and measured engine speed N as well as a model for parts of the intake system.

4.1   Air Intake System Modeling

Given the engine speed and the pressure in the intake manifold, the air-mass flow to the cylinder can be estimated. There is considerable pressure dynamics in the intake manifold and this can be described by a model. Measured signals are used as input to the model. A summary of available sensors and a system overview are given in Figure 4.1.

The intake manifold model is described in three steps starting with the most interesting; air-mass flow to the cylinder, air-mass flow into the manifold, and finally the intake manifold pressure dynamics. For a description of the subscripts and symbol names, please see the nomenclature in Appendix A.1.

4.1.1   Air-Mass Flow into Cylinder

A standard method to model air-mass-to-cylinder (Heywood, 1988; Taylor, 1994) and a variant of (Tseng and Cheng, 1999) is discussed in their capability of describing air-mass-to-cylinder and intake manifold pressure for different positions of the wastegate. At the end a new interpretation of air-mass-to-cylinder is presented, which combines both methods.
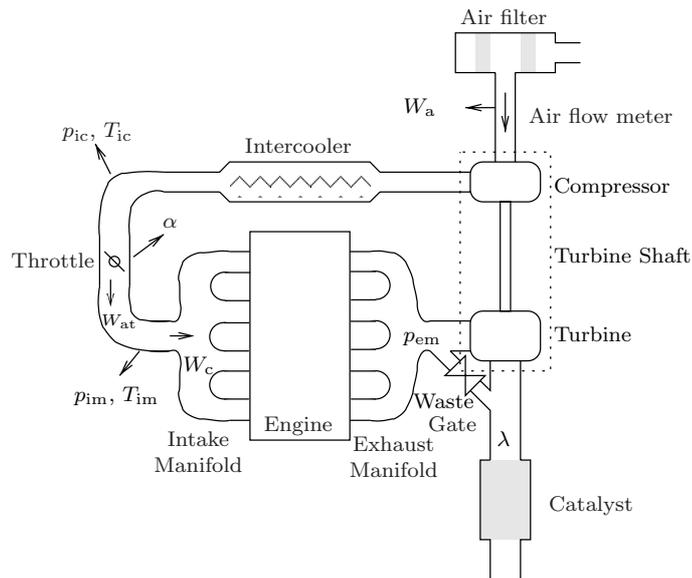
Figure 4.1: The air-mass flow after the air-filter is measured by a hot-film air-mass flow sensor, W_a. An intercooler cools the air and there are sensors for pressure, p_{ic}, and temperature T_{ic}. The throttle governs the air-mass flow into the manifold and is operated by setting the angle of the throttle plate, α. The air-mass flow past the throttle is W_{at} and the air-mass flow to the cylinders is W_c. In the intake manifold there are two sensors, one for pressure p_{im} and one for temperature T_{im}. The wastegate is controlled by a pneumatic system via a pulse width modulated (PWM) signal from the engine control system, or it can be manually opened by a handle.

Air-Mass-to-Cylinder Using Mapped Volumetric Efficiency

A standard method to calculate air-mass flow into the cylinder is to use the volumetric efficiency of the engine η_{vol} (Heywood, 1988; Taylor, 1994). The volumetric efficiency is mapped at steady-state, for a nominal setting of the wastegate, as a function of engine speed N and mean intake manifold pressure p_{im} (Hendricks and Sorensen, 1990). The air-mass flow to the cylinder (Heywood, 1988) is then written as

$$W_{\mathrm{c}std}\left(N, p_{\mathrm{im}}, T_{\mathrm{im}}\right) = \eta_{\mathrm{vol}}\left(N, p_{\mathrm{im}}\right) \frac{p_{\mathrm{im}} V_d}{R_{\mathrm{im}} T_{\mathrm{im}}} \frac{N}{n_r} \tag{4.1}$$

Air-mass-to-cylinder with Modeled Offset in $\eta_{\mathbf{vol}}$

A day-to-day variation in η_{vol} of a few percent in the mapped volumetric efficiency is reported in (Tseng and Cheng, 1999). Their solution to the problem is to model this as an additive offset in volumetric efficiency $\Delta\eta_{\mathrm{vol}}$

$$W_{\mathrm{c}_{\mathrm{ts}}}(N, p_{\mathrm{im}}, T_{\mathrm{im}}, \Delta\eta_{\mathrm{vol}}) = \left(\eta_{\mathrm{vol}}\left(N, p_{\mathrm{im}}\right) + \Delta\eta_{\mathrm{vol}}\right) \frac{p_{\mathrm{im}} V_d}{R_{\mathrm{im}} T_{\mathrm{im}}} \frac{N}{n_r} \tag{4.2}$$

The additive offset $\Delta\eta_{\mathrm{vol}}$ is assumed to be more slowly varying than other dynamics, i.e. it is modeled as a constant by $\frac{\mathrm{d}\Delta\eta_{\mathrm{vol}}}{\mathrm{d}t} = 0$. By proper selection of $\Delta\eta_{\mathrm{vol}}$ this approach is suited to adapt to the changing volumetric efficiency for different wastegate settings.

Air-Mass Flow to Cylinder With Air-Mass-Offset

For nominal wastegate position the expected air-mass to cylinder is well described by the model in Equation (4.1). However when the wastegate is operated the volumetric efficiency changes and this phenomena is caused by a change in exhaust manifold pressure. In Equation (4.2) the offset in volumetric efficiency $\Delta\eta_{\mathrm{vol}}$ can be interpreted as an air-mass-offset.

$$W_{\mathrm{c}_{\mathrm{ts}}} = \underbrace{\eta_{\mathrm{vol}}\left(N, p_{\mathrm{im}}\right) \frac{p_{\mathrm{im}} V_d}{R_{\mathrm{im}} T_{\mathrm{im}}} \frac{N}{n_r}}_{W_{\mathrm{c}std}} + \underbrace{\Delta\eta_{\mathrm{vol}} \frac{p_{\mathrm{im}} V_d}{R_{\mathrm{im}} T_{\mathrm{im}}}}_{\text{Air mass offset}} \frac{N}{n_r} \tag{4.3}$$

The in-cylinder air-mass-offset (m_Δ), in Equation (4.3) is the difference of the expected air-mass through η_{vol} in Equation (4.1) and the current air-mass flow. The air-mass flow to the cylinder can then be written as a sum of air-mass-to-cylinder expected from Equation (4.1) and the in-cylinder air-mass offset m_Δ

$$W_{\mathrm{c}}\left(N, p_{\mathrm{im}}, T_{\mathrm{im}}, p_{\mathrm{em}}, (A/F), \ldots\right) =$$
$$W_{\mathrm{c}std}\left(N, p_{\mathrm{im}}, T_{\mathrm{im}}\right) + m_\Delta\left(p_{\mathrm{em}}, p_{\mathrm{im}}, (A/F), \ldots\right) \frac{N}{n_r} \tag{4.4}$$

In Equation (4.4) the in-cylinder air-mass-offset m_Δ is sensitive to the exhaust manifold pressure, the air/fuel ratio, and the dots in Equation (4.4) represent other influences including model errors.

4.1.2 Air-Mass Flow Into the Intake Manifold

On the modeled engine the sensor for air-mass flow is located after the air filter and the volume between the intake manifold and the sensor is considerable. Instead of using models for the dynamics between the sensor and the throttle a model of the throttle is used instead to improve the estimation of air-mass flow into the intake manifold W_{at}

$$W_{\text{at}}\left(\alpha, p_{\text{im}}, p_{\text{ic}}, T_{\text{ic}}\right) = \frac{p_{\text{ic}}}{\sqrt{R_{\text{im}} T_{\text{ic}}}} A_{\text{eff}}\left(\alpha\right) \Psi\left(p_r\right) \tag{4.5a}$$

$$p_r = \frac{p_{\text{im}}}{p_{\text{ic}}} \tag{4.5b}$$

$$A_{\text{eff}}\left(\alpha\right) = A\left(\alpha\right) C_d\left(\alpha\right) = e^{c_2\alpha^2 + c_1\alpha + c_0} \tag{4.5c}$$

$$\Psi\left(p_r\right) = \begin{cases} \sqrt{\frac{2\gamma}{\gamma-1}\left(p_r^{\frac{2}{\gamma}} - p_r^{\frac{\gamma+1}{\gamma}}\right)} & \text{for } p_r > \left(\frac{2}{\gamma+1}\right)^{\frac{\gamma}{\gamma-1}} \\ \sqrt{\frac{2\gamma}{\gamma-1}\left(\left(\frac{2}{\gamma+1}\right)^{\frac{2}{\gamma-1}} - \left(\frac{2}{\gamma+1}\right)^{\frac{\gamma+1}{\gamma-1}}\right)} & \text{otherwise} \end{cases} \tag{4.5d}$$

The $\Psi\left(p_r\right)$ governs the flow through the restriction depending on the pressure ratio p_r, Equation (4.5b). The function $A_{\text{eff}}\left(\alpha\right)$ is a product of the area $A\left(\alpha\right)$, and discharge coefficient $C_d\left(\alpha\right)$ (Nyberg and Nielsen, 1997) but with a different parameterization. The parameters are fitted in least square sense to mapped engine data. In Figure 4.2 the result of the modeled $A_{\text{eff}}\left(\alpha\right)$ is shown. A systematic relative error is present in the bottom right corner of Figure 4.2. The relative error is positive for large p_r which indicates that $A_{\text{eff}}\left(\alpha\right)$ could be slightly improved by including p_r, which is supported in (Krysander, 2000). At large throttle plate angles (high intake manifold pressures) there are also systematic errors in $A_{\text{eff}}(\alpha)$ which can be reduced by introducing p_{im} in the area function (Arsie et al., 1996). The errors for this throttle model is in the same magnitude as in (Müller et al., 1998) where an accuracy of $\pm 4\%$ is mentioned. The effective area estimation with this parameterization is performed with a resolution of $\pm 6\%$.

In Equation (4.5a) both the pressure p_{ic} and the temperature T_{ic} before the throttle is needed. Measurements can be used since the dynamics of p_{ic} and T_{ic} is considerably slower than p_{im}, due to the substantially larger volume of the system before the throttle and to the slow dynamics of the compressor. The measurements of p_{ic} and T_{ic} are also subjected to lower pumping noise.
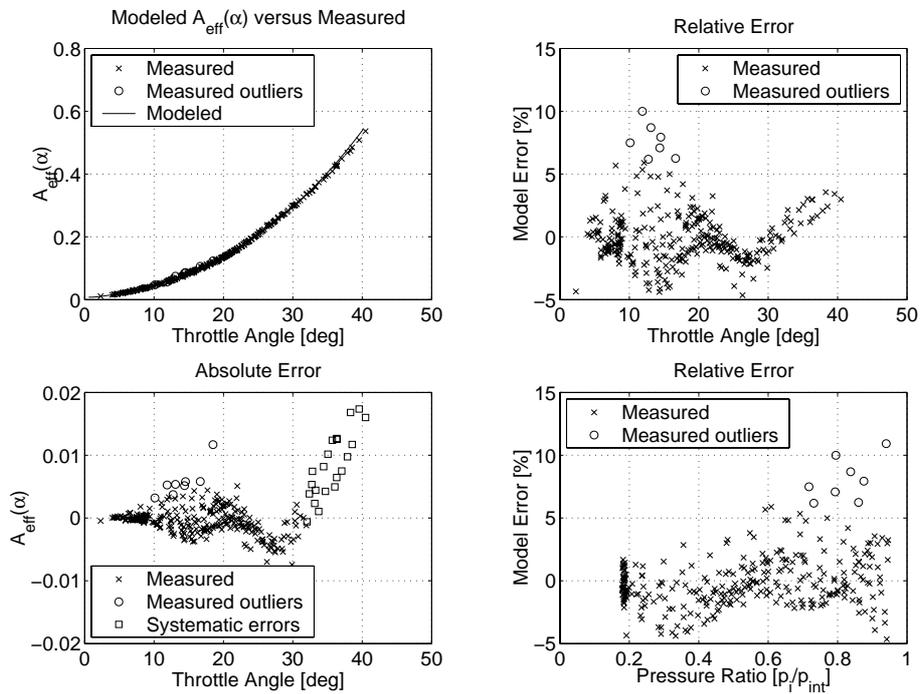
Figure 4.2: Comparison of measured and calculated $A_{\mathrm{eff}}(\alpha)$. The fit is within 6% for most points. The absolute and relative errors are shown as a function of throttle angle and note that the errors are spread equally around zero except for large α. In the bottom right corner the relative error as a function of pressure ratio is shown.

4.1.3 Intake Manifold Pressure Dynamics

To model intake manifold pressure dynamics standard assumptions (Hendricks and Sorensen, 1990) have been made: Ideal gas, and mass conservation in the intake manifold. The pressure change inside the volume (V_{im}) of the intake manifold can now be written, where $K_{\text{im}} = \frac{R_{\text{im}} T_{\text{im}}}{V_{\text{im}}}$, as

$$\frac{\mathrm{d}p_{\text{im}}}{\mathrm{d}t} = K_{\text{im}} \left(W_{\text{at}} \left(\alpha, p_{\text{im}}, p_{\text{ic}}, T_{\text{ic}} \right) - W_{\text{c}} \right) \tag{4.6}$$

In Equation (4.6) W_{c} can be any of the described air-mass-to-cylinder flows. The flow into the manifold is described by a model of the throttle, Equation (4.5a). Stationary the air-mass flow into the intake manifold W_{at} is the same as the measured air-mass flow W_{a}. The estimated air-mass flow into the manifold $W_{\text{at}} \left(\alpha, p_{\text{im}}, p_{\text{ic}}, T_{\text{ic}} \right)$ may differ from the measured air-mass flow W_{a}, even stationary, due to model errors. To decrease the effect of throttle model errors, observers for air-mass-through throttle have been proposed in e.g. (Jensen et al., 1997). As the behavior of speed-density based air-mass-to-cylinder observers is studied here especially in their ability to fulfilling the mass balance in Equation (4.6) stationary, the throttle model error is neglected.

Temperature dynamics is also present in the intake manifold during large pressure transients (Chevalier et al., 2000). In this study temperature dynamics is neglected as the pressure change caused by a wastegate transient is small. When the engine is running at steady-state, the temperature after a pressure transient is unchanged and therefore the added complexity of temperature dynamics is unnecessary.

4.2 Aim of Test of Observers

Speed-density methods are based on a fast pressure sensor in the intake manifold, and thus a promising method to handle fast transients. Speed-density methods has therefore been chosen as the focus of the observer investigation. Stationary correct mass-balance can be easily added by using the slower air-mass flow sensor as argued above.

4.2.1 Test Conditions for the Observers

At stationarity the air-mass flow to the cylinder is the same as the air-mass flow through the throttle, W_{at}. This is used to study steady-state air-mass-to-cylinder estimation for the observers in Sections 4.3.1, 4.3.2, and 4.3.3. The test data is measured at 3100 RPM and at a bmep of 5.3 bar. The engine is equipped with an air-mass controller which objective is to maintain constant air-mass flow. Here the performed experiment is to open and close the wastegate with a constant reference air-mass flow and it is shown in Figure 4.3. To achieve wastegate steps of high amplitude a manual control device is used instead of

the production vacuum control actuator. When the wastegate is opened there is an air-mass flow transient at time 5 seconds. A second air-mass flow transient is present when the wastegate is closed at time 21 seconds. What is furthermore interesting is that the mapped volumetric efficiency does not match the calculated when the wastegate is open. This shows up as a 3% steady-state difference between the mapped and measured volumetric efficiency in the bottom of Figure 4.3. The cause is that the volumetric efficiency is sensitive to changes in residual gases in the cylinder, which depends on the pressure ratio $\frac{p_{\text{im}}}{p_{\text{em}}}$ (Heywood, 1988; Taylor, 1994).

4.3   Air-Mass to Cylinder Observers

The air-mass-to-cylinder can be calculated using the engine speed and intake manifold pressure. Here the air-mass-to-cylinder is estimated in three different ways and all of the observers rely on feed-back from the fast pressure sensor. First, by observing the intake manifold pressure, the air-mass to-cylinder flow is estimated by applying Equation (4.1). The second method estimates air-mass-to-cylinder using the model in Equation (4.2), where the intake manifold pressure is observed together with an offset in volumetric efficiency $\Delta\eta_{\text{vol}}$. Finally an observer that estimates air-mass-to-cylinder by observing the intake manifold pressure and the in-cylinder air-mass-offset m_{Δ} is presented. It estimates air-mass-to-cylinder using Equation (4.4).

In the observers the following measurement signals are used: Engine speed N, pressure before the throttle p_{ic}, temperature before the throttle T_{ic}, throttle plate angle α, intake manifold pressure p_{im}, and intake manifold temperature T_{im}.

4.3.1   Observer with Proportional Feedback

A constant gain extended Kalman filter (CGEKF) (Safanov and Athans, 1978) for the intake manifold pressure, Equation (4.6), with proportional feedback from the intake manifold pressure sensor, is suggested in (Hendricks et al., 1992). In Equation (4.6) $W_{\text{c}} = W_{\text{c}_{\text{std}}}(N, \hat{p}_{\text{im}}, T_{\text{im}})$ and the mass flow into the intake manifold is given by Equation (4.5a). The CGEKF methodology results in the following observer for the intake manifold pressure

$$\frac{\mathrm{d}\hat{p}_{\text{im}}}{\mathrm{d}t} = K_{\text{im}}\left(W_{\text{at}}\left(\alpha, \hat{p}_{\text{im}}, p_{\text{ic}}, T_{\text{ic}}\right) - W_{\text{c}_{\text{std}}}\left(N, \hat{p}_{\text{im}}, T_{\text{im}}\right)\right) + K_{\text{obs}}\left(p_{\text{im}} - \hat{p}_{\text{im}}\right)$$

$$(4.7)$$
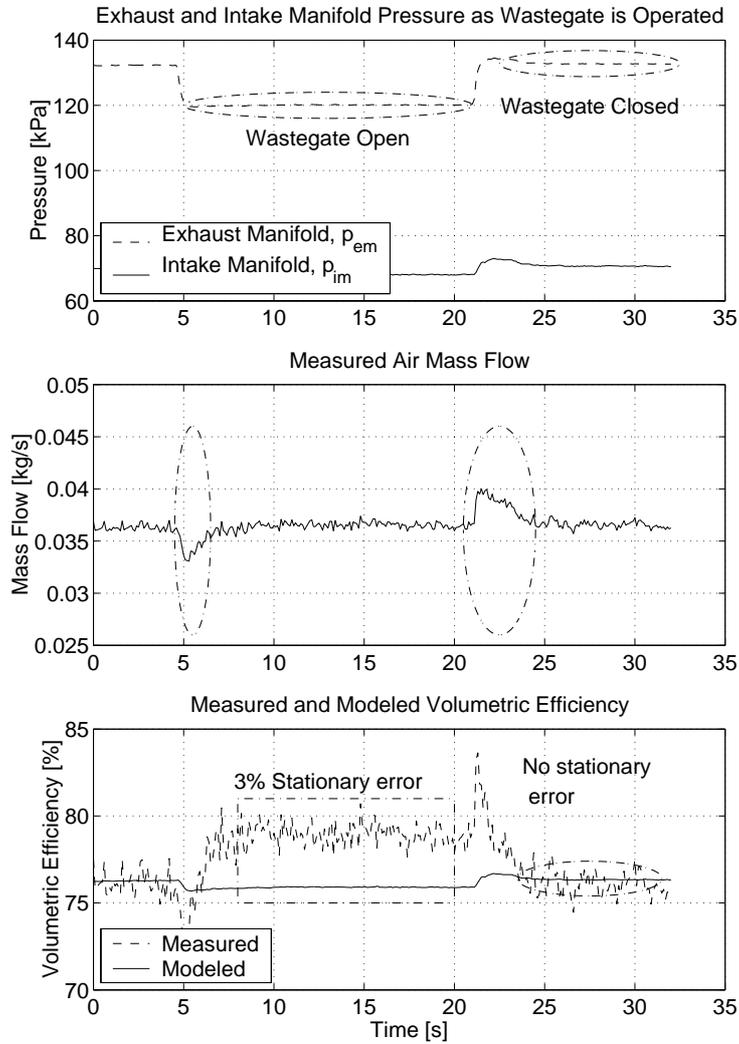
Figure 4.3: Air-mass flow data, measured at 3100 RPM and 5.3 bar brake mean effective pressure during a step in wastegate. *Top:* Exhaust pressure drops when the wastegate is opened at time 5 and it increases again when the wastegate is closed at time 21 seconds. *Center:* Measured air-mass flow is controlled to a constant value during the experiment except for the transients caused by the opening and closing of the wastegate which disturbs the controller. The air-mass flow is constant when the controller has converged regardless of wastegate position. *Bottom:* The volumetric efficiency increases as the wastegate is opened. At most there is a 3% steady-state error, compared to the mapped value.

Tuning

When K_{obs} is calculated in Equation (4.7), the variance of the state noise of $\hat{p}_{\mathrm{im}}$ is assumed to be the first harmonic of the pumping noise (Hendricks et al., 1992). The variance of the measurement signal p_{im} is measured with the engine off but with ignition and dynamometer on. No dependence between the measurement variance and the state variances is assumed. K_{obs} depends on the current state of the engine (N, p_{im}) and can be stored in a table.

Steady-State Properties

How does this type of observer handle the effect of a change in wastegate position? As shown in Figure 4.3 the volumetric efficiency changes slightly during the wastegate step. The impact on estimated air-mass-to-cylinder and intake manifold pressure is theoretically studied here. When $\frac{\mathrm{d}\hat{p}_{\mathrm{im}}}{\mathrm{d}t} = 0$ the observer has converged and this occurs when either $W_{\mathrm{at}}\left(\alpha, \hat{p}_{\mathrm{im}}, p_{\mathrm{ic}}, T_{\mathrm{ic}}\right) = W_{\mathrm{c_{std}}}(N, \hat{p}_{\mathrm{im}}, T_{\mathrm{im}})$, which is the case when the volumetric efficiency is correct, or when there is a steady-state error in estimated pressure. In the later case there is an error in the volumetric efficiency. By setting the left hand side of Equation (4.7) to zero and solve for the stationary pressure difference $(p_{\mathrm{im}} - \hat{p}_{\mathrm{im}})$ two interesting properties of this observer are revealed.

$$(p_{\mathrm{im}} - \hat{p}_{\mathrm{im}}) = -\frac{K_{\mathrm{im}}}{K_{\mathrm{obs}}} \underbrace{\left(W_{\mathrm{at}}\left(\alpha, \hat{p}_{\mathrm{im}}, p_{\mathrm{ic}}, T_{\mathrm{ic}}\right) - \hat{W}_{\mathrm{c_{std}}}\left(N, \hat{p}_{\mathrm{im}}, T_{\mathrm{im}}\right)\right)}_{\neq 0} \qquad (4.8)$$

When there is a steady-state error in estimated pressure the error decreases as the gain K_{obs} increases. A steady-state pressure estimation error also corresponds to a not fulfilled mass balance in Equation (4.6). The difference in mass balance $W_{\mathrm{at}}\left(\alpha, \hat{p}_{\mathrm{im}}, p_{\mathrm{ic}}, T_{\mathrm{ic}}\right) - W_{\mathrm{c_{std}}}(N, \hat{p}_{\mathrm{im}}, T_{\mathrm{im}})$ is:

$$\left(W_{\mathrm{at}}\left(\alpha, \hat{p}_{\mathrm{im}}, p_{\mathrm{ic}}, T_{\mathrm{ic}}\right) - W_{\mathrm{c_{std}}}(N, \hat{p}_{\mathrm{im}}, T_{\mathrm{im}})\right) = -\frac{K_{\mathrm{obs}}}{K_{\mathrm{im}}}\left(p_{\mathrm{im}} - \hat{p}_{\mathrm{im}}\right) \qquad (4.9)$$

Here the estimate of air-mass-to-cylinder is correct when the wastegate is at nominal position, which is the case during engine mapping. When the wastegate opens, the steady-state error in the estimated air-mass-to-cylinder is proportional to the feed-back gain. This is illustrated in Equation (4.9), where the stationary air-mass estimation error $(W_{\mathrm{at}}\left(\alpha, \hat{p}_{\mathrm{im}}, p_{\mathrm{ic}}, T_{\mathrm{ic}}\right) - W_{\mathrm{c_{std}}}(N, \hat{p}_{\mathrm{im}}, T_{\mathrm{im}}))$ increases with the feed-back gain. To estimate the same air-mass-to-cylinder as the air-mass flow through the throttle, for various settings of the wastegate, the gain must be set to zero. For the estimated intake manifold pressure a high feed-back gain results in a small stationary intake manifold pressure estimation error and a fast pressure estimation. A side effect is that there is no mass balance in Equation (4.6). This means that the observer does not estimate the same air-mass-to-cylinder as the mass flow through the throttle. The results is that

it is impossible with only proportional feed-back to get correct pressure and air-mass-to-cylinder estimation for an engine with wastegate. The pressure error for a low and a high feed-back gain is then shown in Figure 4.4. For the lower gain the estimation error in intake manifold pressure is larger when the wastegate is opened. Finally the difference $(W_{\text{at}}(\alpha, \hat{p}_{\text{im}}, p_{\text{ic}}, T_{\text{ic}}) - W_{\text{c}_{\text{std}}}(N, \hat{p}_{\text{im}}, T_{\text{im}}))$ is shown in Figure 4.4. Here the low gain estimates the air-mass-to-cylinder with the least error compared to the estimated air-mass flow through the throttle. For the high gain the error in estimated air-mass-to-cylinder is 2.5% compared to the estimated air-mass flow into the intake manifold when the wastegate is open.

4.3.2 Air-mass-to-cylinder Observer with Additive Offset in η_{vol}

A method capable of handling offsets in volumetric efficiency is developed in (Tseng and Cheng, 1999). It uses integration to estimate the offset in η_{vol} which cancels the steady-state error in the intake manifold pressure estimate. A minor modification has been made to make the method time continuous by substituting sums to integrations. The model of the air-mass flow into the cylinder is Equation (4.2) and the air-mass flow into the intake manifold is estimated by Equation (4.5a). Intake manifold pressure dynamics is given by Equation (4.6) with $W_{\text{c}} = W_{cts}\left(N, \hat{p}_{\text{im}}, T_{\text{im}}, \hat{\Delta\eta}_{\text{vol}}\right)$. In the model the $\Delta\eta_{\text{vol}}$ is constant and the resulting observer they present is

$$\frac{\text{d}\hat{p}_{\text{im}}}{\text{d}t} = K_{\text{im}}\left(W_{\text{at}}\left(\alpha, \hat{p}_{\text{im}}, p_{\text{ic}}, T_{\text{ic}}, \hat{\Delta\eta}_{\text{vol}}\right) - W_{\text{c}_{\text{ts}}}(N, \hat{p}_{\text{im}}, T_{\text{im}})\right) \qquad (4.10)$$

$$\frac{\text{d}\hat{\Delta\eta}_{\text{vol}}}{\text{d}t} = -\frac{1}{L_1}\frac{\left(\eta_{\text{vol}}(N, \hat{p}_{\text{im}}) + \hat{\Delta\eta}_{\text{vol}}\right)^2 NV_d}{R_{\text{im}}T_{\text{im}}W_{\text{at}}(\alpha, \hat{p}_{\text{im}}, p_{\text{ic}}, T_{\text{ic}})n_r}(p_{\text{im}} - \hat{p}_{\text{im}}) \qquad (4.11)$$

In Equation (4.10) no feed-back from the measured intake manifold pressure is used and the feed-back gain in Equation (4.11) is from (Tseng and Cheng, 1999).

Tuning

The convergence rate of the estimation of $\Delta\eta_{\text{vol}}$ in Equation (4.11) is controlled by a scaling factor L_1. No systematic tuning method for L_1 is presented in (Tseng and Cheng, 1999).

Steady-State Properties

When the observer has converged, Equation (4.11), is zero and the estimated intake manifold pressure is equal to the measured. Air-mass flow to cylinder $W_{\text{c}_{\text{ts}}}$ must now equal the estimated air-mass flow into the intake manifold
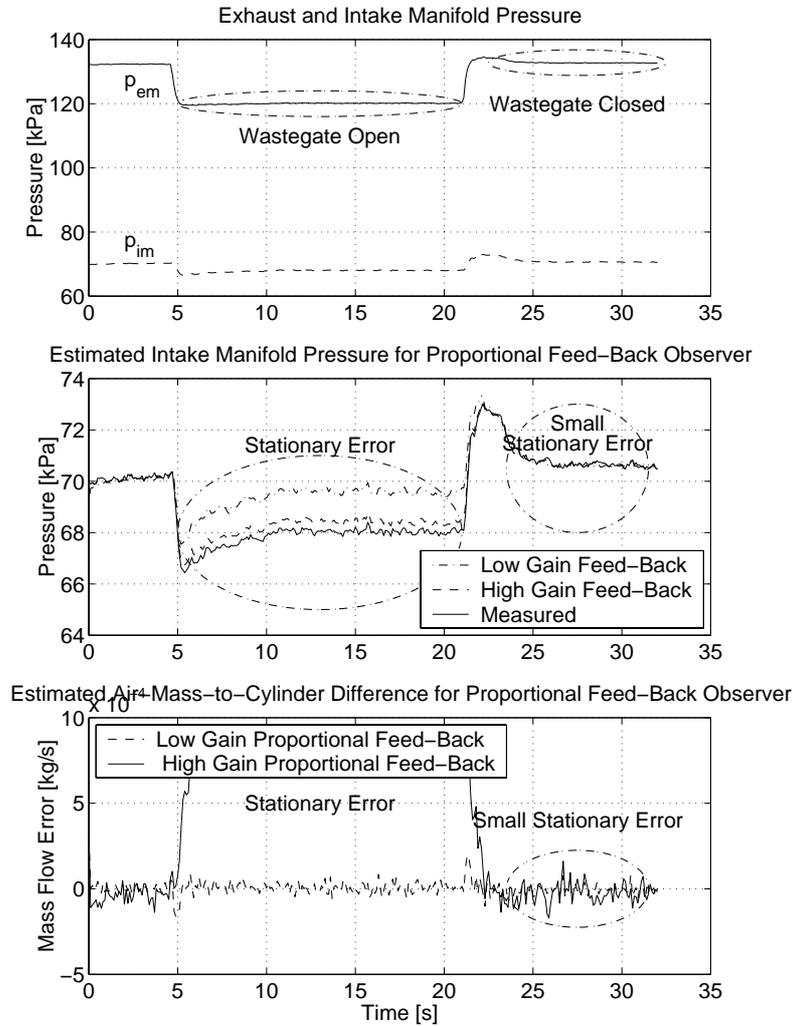
Figure 4.4: *Top:* The wastegate is open between time 5 and 21 seconds. *Center:* For closed wastegate, where the description of η_{vol} is correct, the stationary error in the observed intake manifold pressure is independent of the feed-back gain. When the wastegate is open the error is inversely proportional to the feed-back gain. *Bottom:* In the estimated air-mass-to-cylinder there is a stationary error present when the wastegate is open. For the high gain the error is 2.5%. For the low gain the estimated air-mass is the same as the air-mass-through the throttle.

$W_{\text{at}}(\alpha, \hat{p}_{\text{im}}, p_{\text{ic}}, T_{\text{ic}})$ in order for the intake manifold pressure to be constant. Therefore this observer will give correct stationary estimates of the air-mass-to-cylinder. Measurements in Figure 4.5 support this where there are two transients in the difference between the estimated air-mass flow through the throttle and estimated air-mass-to-cylinder which is caused by the operations of the wastegate. Another feature of this observer is that it estimates correct stationary intake manifold pressure, after the wastegate has been operated, which is shown in Figure 4.5. This means that when the estimated intake manifold pressure equals the measured the estimated air-mass-to-cylinder is equal to $W_{\text{at}}(\alpha, \hat{p}_{\text{im}}, p_{\text{ic}}, T_{\text{ic}})$. A problem is reported during intake manifold pressure transients (Tseng and Cheng, 1999) where the observer updates $\Delta\eta_{\text{vol}}$ incorrectly. To solve this problem the adaption is turned off for large pressure transients. As the pressure transients are small during changes in wastegate position there is no need in this case to turn off the adaption. In Figure 4.5 these properties are shown for a step in wastegate position.

4.3.3 Observer With Air-Mass-Offset Estimation

A change in wastegate position results in a changed air-mass flow to the cylinder. In the proposed model in Section 4.1.1 this in-cylinder air-mass-offset is called m_Δ and it is the cause of the change in volumetric efficiency. Now denote the estimated in-cylinder air-mass-offset $\hat{m}_\Delta$. If $\hat{m}_\Delta$ is assumed to be slowly varying it can be estimated together with the intake manifold pressure, Equation (4.6), using CGEKF-theory. The information of $\hat{m}_\Delta$ is then used in the calculation of air-mass-to-cylinder. In Equation (4.6) $W_{\text{c}} = W_{\text{c}_{\text{std}}}(N, \hat{p}_{\text{im}}, T_{\text{im}}) + \hat{m}_\Delta \frac{N}{n_r}$ and the air-mass flow into the manifold is given by Equation (4.5a)

$$
\frac{\mathrm{d}\hat{p}_{\text{im}}}{\mathrm{d}t} =
$$

$$
- K_{\text{im}} \left(\underbrace{\overbrace{\eta_{\text{vol}}(N, \hat{p}_{\text{man}}) \frac{\hat{p}_{\text{im}} V_d N}{R_{\text{im}} T_{\text{im}} n_r}}^{\text{Expected air mass}} + \overbrace{\frac{N}{n_r} \hat{m}_\Delta}^{\text{Offset}}}_{\text{Air mass flow to cylinder}} - W_{\text{at}}(\alpha, \hat{p}_{\text{im}}, p_{\text{ic}}, T_{\text{ic}}) \right) +
$$

$$
K_1 \left(p_{\text{im}} - \hat{p}_{\text{im}} \right) \quad \text{(4.12a)}
$$

$$
\frac{\mathrm{d}\hat{m}_\Delta}{\mathrm{d}t} = K_2 \left(p_{\text{im}} - \hat{p}_{\text{im}} \right) \quad \text{(4.12b)}
$$

Tuning

The observer is tuned by linearizing Equation (4.12a) and determining the observer gains K_1 and K_2 by applying Kalman filtering technique. The covariance matrices used in the Kalman filter are calculated as follows. The intake pressure state variance is assumed to be the first harmonics of the intake manifold pumping (Hendricks et al., 1992). In measurements the amplitude of the pumping are
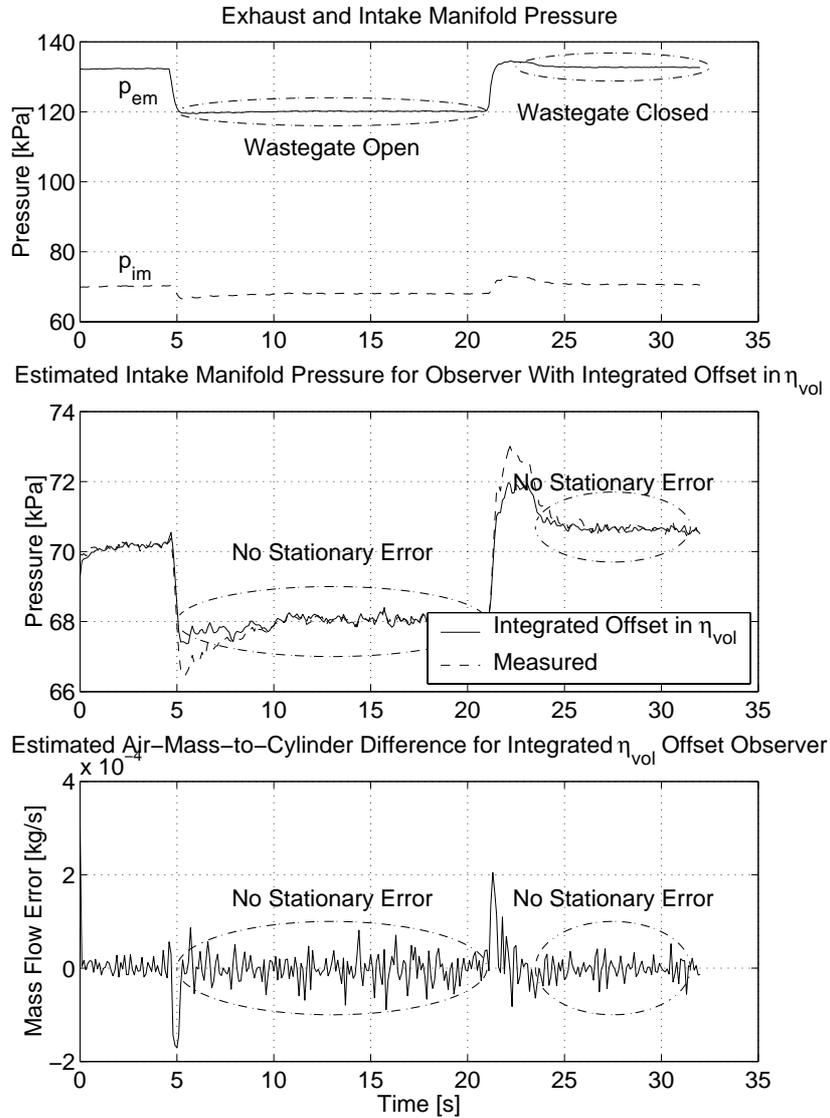
Figure 4.5: *Top:* The wastegate is open between time 5 and 21 seconds. *Center:* Observed intake manifold pressure tracks the measured intake manifold pressure excellently for stationary conditions. *Bottom:* The estimated air-mass-to-cylinder is equal to the estimated air-mass flow through the throttle.

less or approximately equal to 10% of the measured mean intake manifold pressure resulting in a variance of $\frac{1}{2 \cdot 10} p_{\mathrm{im}}$. The variance of the in-cylinder air-mass-offset m_Δ is based on calculated residual gas variance when the exhaust pressure varies sinusoidally. Its peak-to-peak amplitude is the exhaust pressure difference caused by an opening and closing of the wastegate. When it is open the exhaust manifold pressure is approximately equal to the ambient pressure. The residual gas mass is calculated using the approximative model in (Heywood, 1988)

$$x_r = \left(1 + \frac{T_r}{T_{\mathrm{im}}} \left(r_c \left(\frac{p_{\mathrm{im}}}{p_{\mathrm{em}}} \right) - \left(\frac{p_{\mathrm{im}}}{p_{\mathrm{em}}} \right)^{(\gamma-1)/\gamma} \right) \right)^{-1} \tag{4.13}$$

$$T_1 = T_r r_c x_r \left(\frac{p_{\mathrm{im}}}{p_{\mathrm{em}}} \right) \tag{4.14}$$

$$m_r = \frac{x_r}{1 - x_r} \frac{p_{\mathrm{im}} V_d}{R_{\mathrm{im}} T_{\mathrm{im}}} \left(1 + \frac{1}{\lambda \left(\frac{A}{F} \right)_s} \right) \tag{4.15}$$

The following values were used in Equations (4.13,4.14,4.15): $T_r = 1400$, η_{vol} from the engine map, and $\lambda = 1$. Simulations are used to estimate the variance of m_r. Further, the intake manifold pressure and air-mass-offset are assumed to be independent. The same measurement noise is used as in the calculations of the feedback gain in the observer with only proportional feedback. K_1 and K_2 depends on the current state of the engine (N, p_{im}) and can be stored in a table.

Properties

The convergence rate can be set by the proportional feed-back and the integrating part cancels the stationary error since Equation (4.12b) is only zero when the estimated pressure is equal to the measured. A systematic tuning method also was proposed in Section 4.3.3 which makes use of a standard methodology. The rate of convergence depends on the covariance matrices where all but the mass offset variance is measurable.

In order for the air-mass offset $\hat{m}_\Delta$ to converge, the measured and estimated intake manifold pressure must be the equal, Equation (4.12b). When the mass offset $\hat{m}_\Delta$ has converged the feed-back term $K_1 (p_{\mathrm{im}} - \hat{p}_{\mathrm{im}})$ in Equation (4.12a) is zero and this leaves the mass difference $W_{\mathrm{c_{std}}}(N, \hat{p}_{\mathrm{im}}, T_{\mathrm{im}}) + \hat{m}_\Delta \frac{N}{n_r} - W_{\mathrm{at}} \left(\alpha, \hat{p}_{\mathrm{im}}, p_{\mathrm{ic}}, T_{\mathrm{ic}}, \Delta\hat{\eta}_{\mathrm{vol}} \right)$ to be zero. This means that the 2-state observer also estimates correct intake manifold pressure, and the same air-mass-to-cylinder as the air-mass flow through the throttle, $W_{\mathrm{at}} \left(\alpha, \hat{p}_{\mathrm{im}}, p_{\mathrm{ic}}, T_{\mathrm{ic}}, \Delta\hat{\eta}_{\mathrm{vol}} \right)$. This is illustrated in Figure 4.6.
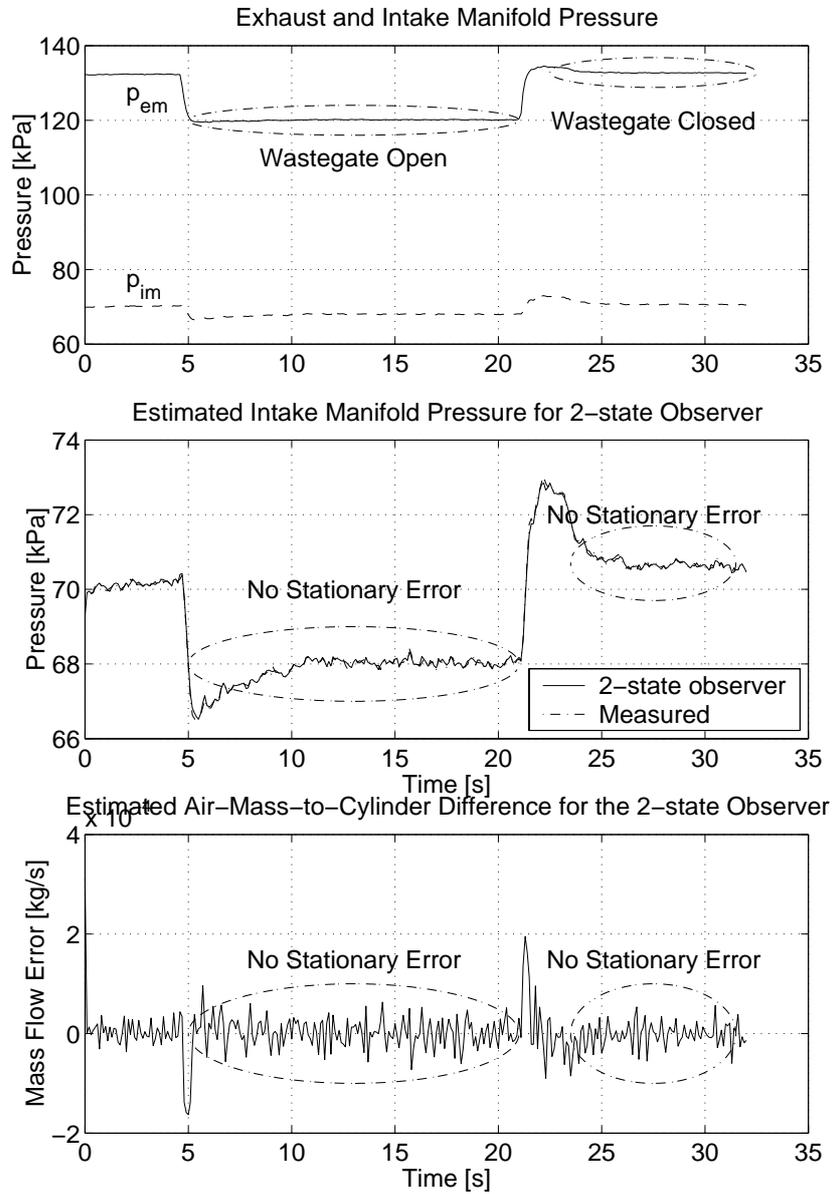
Figure 4.6: *Top:* The wastegate is open between time 5 and 21 seconds. *Center:* Observed intake manifold pressure tracks the measured intake manifold pressure excellently for stationary conditions. *Bottom:* The estimated air-mass-to-cylinder is equal to the estimated air-mass flow through the throttle for stationary conditions.

4.4 Results

Observers for estimating air-mass flow to the cylinders, for control of air/fuel ratio, have been studied on a turbocharged SI-engine with wastegate. The study has focused on properties for the fast speed-density air-mass-estimation principle, since the ability to fulfill mass-balance stationary can be added using feed-back from air-mass flow sensor. It was demonstrated that methods relying on proportional feed-back from the intake manifold pressure sensor is unable to estimate the system state. For this observer the feed-back gain is a trade-off between fast pressure convergence or accurate stationary air-mass-to-cylinder estimation. A high gain results in fast pressure convergence but a large air-mass-to-cylinder estimation error. Better steady-state estimates of air-mass-to-cylinder is achieved using models with an additional state. The observers for these models are the observer with volumetric efficiency offset estimation and the 2-state observer. For these observers intake manifold pressure converges to measured intake manifold pressure and they estimate the same mass flow to cylinders as the described air-mass flow into the intake manifold. For the 2-state observer a systematic tuning method is also suggested.

Exhaust Manifold Pressure Estimation

It is desirable to have knowledge about the exhaust manifold pressure, especially in a turbocharged spark ignited (SI) engine with wastegate, where it gives useful information about the turbine and wastegate operation. This information can be utilized by the control and diagnosis systems. Knowledge about the exhaust manifold pressure can also be used for leakage detections. This will be considered in Chapter 6. The exhaust manifold pressure is normally not measured due to the high temperatures in the exhaust system and the extra cost of an additional sensor. Exhaust manifold pressure estimators that extract information from available sensors are therefore desirable.

Observers for pressure and temperature in the exhaust manifold have been proposed and applied with good results for naturally aspirated (NA) SI-engines in (Maloney and Olin, 1998). The exhaust manifold pressure is generated by the exhaust system which acts as a flow restriction. In NA engines this flow restriction can be modeled accurately using only one constant, (Eriksson et al., 2001). On turbocharged engines with wastegate this restriction consists of three parts: the exhaust system which acts as a restriction and produces back pressure, the turbine which also acts as a restriction, and the wastegate which acts as a variable restriction and shunts varying amounts of the exhaust gases past the restricting turbine. Changes in wastegate valve position therefore influence the flow restriction and the exhaust side of the engine can not be considered as a constant flow restriction. In addition the wastegate position is normally not measured, which further complicates the situation.

To estimate the absolute exhaust manifold pressure a simplified thermodynamic model is used. The model relies on information about the air-mass that

enters the cylinder. The air-mass in the cylinder is described by a mean value model of the intake system, like the 2-state observer in Chapter 4 does. No additional sensors in the exhaust system are needed by the estimator after calibration. The only sensors used are air-mass flow, pressure and temperature after the throttle, and these are available on many production engines. The estimated exhaust pressure is only valid under steady-state conditions since a static intake manifold model is used, but it can be extended to describe the exhaust manifold pressure during transients.

5.1   System Overview

In Figure 5.1 the components of the engine and the sensors are shown. For a description of the symbols used, please see the nomenclature in Section A.1. The air enters the air-filter and is then measured by a hot-film air-mass sensor W_a. It is then compressed and cooled by the intercooler. By controlling the throttle plate angle α the air-mass flow into the intake manifold is restricted. The air-mass flow past the throttle and into the intake manifold is W_{at} and in the intake manifold there is one pressure sensor p_{im}, and one temperature sensor T_{im}.

Air-mass flow to the cylinders is denoted W_c and it can not be measured, but at stationary conditions it is equal to W_a. The mass of air that can fill the cylinder depends on, among others, the amount of residual gases in the cylinder. The later is governed by the exhaust manifold pressure p_{em}, which in turn depends on the wastegate position. The ECU normally controls the wastegate but here also a manual device is used to open the wastegate.

5.2   Intake System and Exhaust Pressure Model

Exhaust pressure influences air-mass-to-cylinder through a change in residual gas mass. Changes in residual gas mass can be detected in the intake as a change in volumetric efficiency. A model that describes the influence of exhaust pressure on the intake manifold pressure and air-mass flow is used to estimate the exhaust manifold pressure. The model is a variant of the air-mass to-cylinder model in Chapter 4, which describes changes from a nominal state, by estimating an in-cylinder air-mass offset. The engine is said to run at nominal state when the engine is run at steady state at the same N, p_{im}, and wastegate position as during the mapping of $\eta_{vol}(N, p_{im})$. In the developed exhaust manifold estimator the intake manifold dynamics is neglected.

5.2.1   Air-to-cylinder Model

A standard method to model air-mass-to-cylinder is to map the volumetric efficiency of the engine under stationary conditions (Heywood, 1988; Taylor, 1994). For this model to be correct there is an assumption of constant exhaust
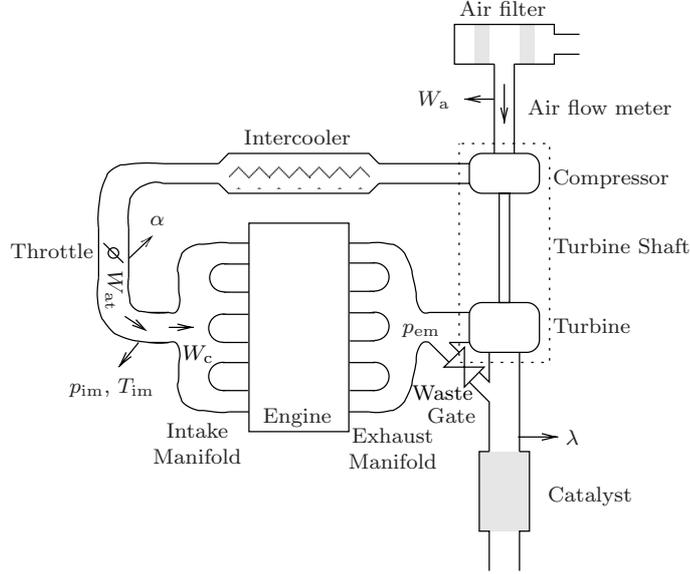
Figure 5.1: Sensors and actuators on the engine. The only measured air-mass flow is before the compressor, W_a.

manifold pressure for that stationary operating point. In a turbocharged engine with wastegate the exhaust manifold pressure can change depending on the setting of the wastegate. The change in exhaust manifold pressure changes the residual gas mass and therefore also the air-mass-to-cylinder which is the same as a change in volumetric efficiency. Air-mass-to-cylinder is well described by the volumetric efficiency as long as the exhaust manifold pressure is the same as during the engine mapping. When the exhaust manifold pressure is the same as during the engine mapping it is referred to as nominal exhaust manifold pressure. When the exhaust pressure is not the same as during the mapping there will be an offset in estimated air-mass compared to the actual air-mass to the cylinder per combustion. The offset is called m_Δ, which can be solved from Equation (4.12a), and at stationarity it is

$$m_\Delta = W_\mathrm{a} \frac{n_r}{N} - \eta_\mathrm{vol}\left(N, p_\mathrm{im}\right) \frac{p_\mathrm{im} V_d}{R_\mathrm{im} T_\mathrm{im}} \tag{5.1}$$

This calculated m_Δ will be used in the derivation of the exhaust manifold pressure estimator. The stationary m_Δ is not valid during intake manifold pressure transients, due to the change in mass inside the intake system. To take the intake manifold dynamics into account the air-mass offset m_Δ could be estimated by the 2-state observer in Chapter 4 using the Equations (4.12a,4.12b), but this will not be used in this chapter.

Here the mapped volumetric efficiency is expressed using a function of engine speed and intake manifold pressure.

$$\eta_{\mathrm{vol}}(N, p_{\mathrm{im}}) = c_0 + c_1 N + c_2 N^2 + c_3 p_{\mathrm{im}}$$

The fit is within 5% for the engine map and intake manifold pressures above 40 kPa.

The influence of the exhaust manifold pressure on volumetric efficiency during changes in wastegate position is shown in Figure 5.2 together with the in-cylinder-air-mass-offset m_Δ. There is a significant increase in m_Δ as the exhaust manifold pressure decreases. This experiment indicates that there is information about the exhaust manifold pressure in the intake system.

5.2.2   Exhaust Pressure Model

The model for the exhaust manifold pressure p_{em} is decomposed into two parts: One is the nominal pressure $p_{\mathrm{em\,nom}}$, measured at nominal wastegate position during the engine mapping. The other is an offset p_{em_Δ} from the nominal conditions which represents the effect of a change in wastegate position. The total model is then written:

$$p_{\mathrm{em}} = p_{\mathrm{em\,nom}} + p_{\mathrm{em}_\Delta} \tag{5.2}$$

At nominal exhaust manifold pressures p_{em_Δ} is zero.

Representation of Nominal Exhaust Pressure

Exhaust pressure during engine mapping $p_{\mathrm{em\,nom}}$ can be expressed either using a map or a polynomial in air-mass flow (Bergström and Brugård, 1999; Pettersson, 2000; Eriksson et al., 2001). Here the back pressure caused by the exhaust system, turbine and nominal setting of the wastegate is expressed as a first order polynomial. In Figure 5.3 the result of the polynomial fit in air-mass flow is shown. In (Bergström and Brugård, 1999) a second order polynomial is used which explained the exhaust manifold pressure very accurate until the wastegate opened. The use of a first order polynomial increases the relative error for low mass flows in Figure 5.3 but it is still sufficiently accurate. To get an estimate of the absolute pressure the ambient pressure p_{a} is added to the expected pressure drop,

$$p_{\mathrm{em\,nom}} = p_{\mathrm{a}} + k_1 W_{\mathrm{at}} + k_2 \tag{5.3}$$

where k_1 and k_2 are tuning constants. For this polynomial in air-mass flow the error is low, less than 4%. As the fit of the polynomial in air-mass flow is a good representation of the nominal exhaust manifold pressure it will be used in the calculations of $p_{\mathrm{em\,nom}}$.
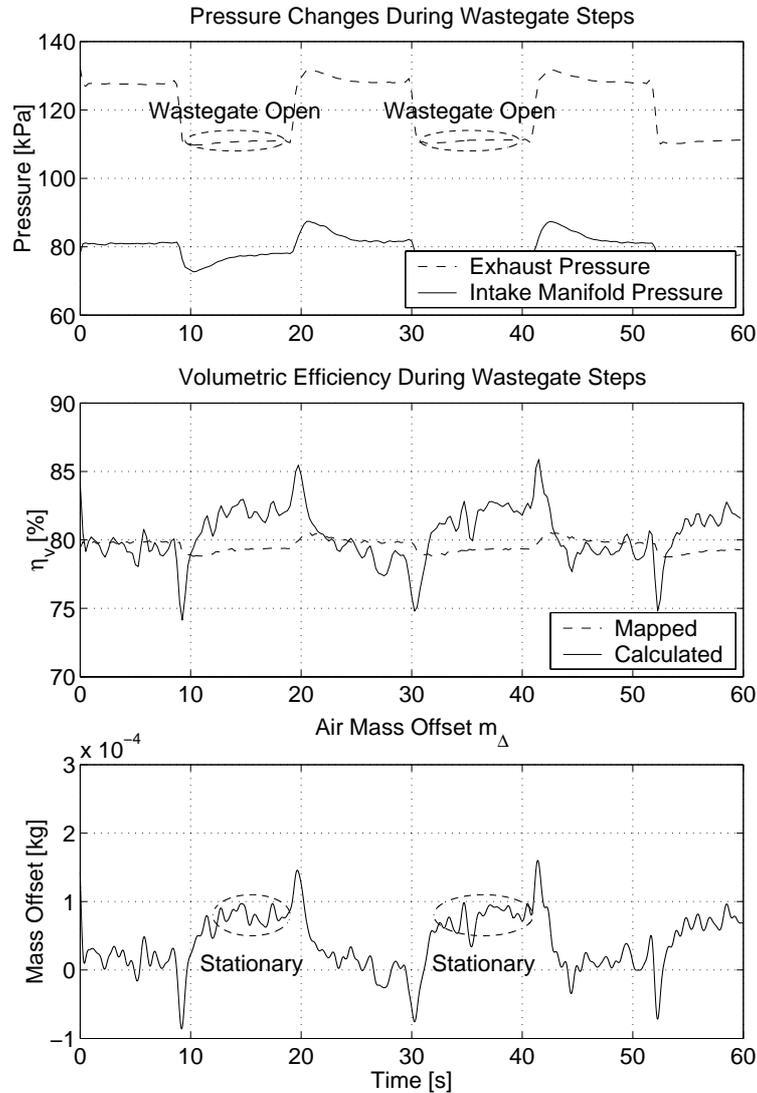
Figure 5.2: Opening and closing of wastegate with air-mass flow controlled to a constant value. *Top:* The exhaust manifold pressure drops for open wastegate. Intake manifold pressure drops only slightly. *Center:* Comparison of calculated, Equation (2.1), volumetric efficiency and mapped. Both are equal for closed wastegate but the volumetric efficiency increases stationary when the wastegate is open. *Bottom:* Offset from expected air-mass m_Δ when the wastegate is open. In the ellipses a stationary in-cylinder air-mass offset is present.
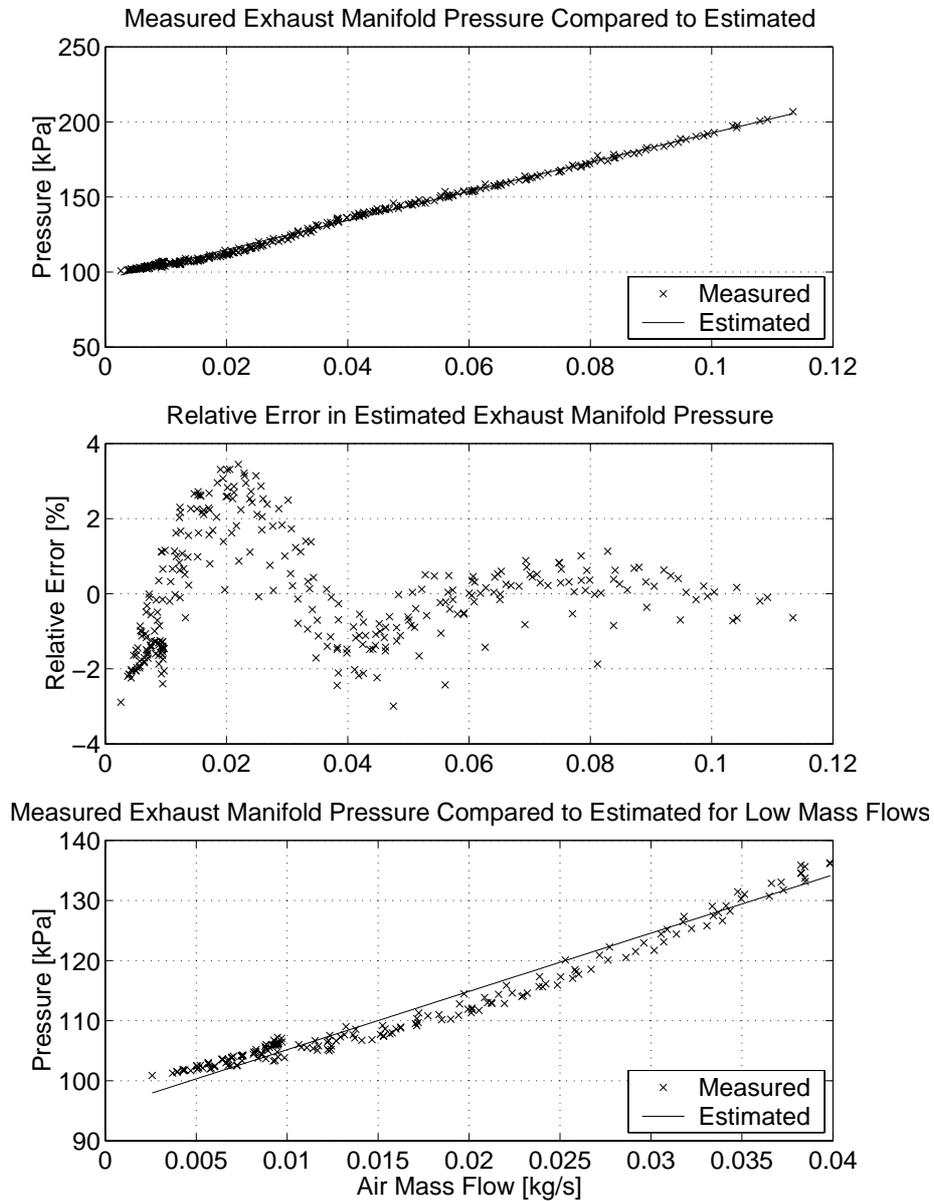
Figure 5.3: *Top:* Exhaust manifold pressure during mapping and fitted first order polynomial in air-mass flow. *Center:* The relative error of the polynomial fitting is less than 4 percent and largest for low mass flows. *Bottom:* For low air-mass flows a second order polynomial would fit better.

Exhaust Manifold Pressure Change

A model for the exhaust manifold pressure is developed, by considering a simplified process for the gas exchange. The simplified gas exchanges includes the assumption that there is no valve overlap and no heat transfer. Furthermore it is assumed that the gases are ideal and that the specific heat for unburned and burned gases are the same, c_v. The mass of gases inside the cylinder at intake valve closing is denoted m and it consists of the mass of air and fuel m_{af} and residual gas mass m_r. With these assumptions, the internal energy of the mixture is conserved according to the first law of thermodynamics which gives

$$mc_vT_1 = m_{af}c_vT_{af} + m_rc_vT_r \tag{5.4a}$$

$$m_{af} = m_a + m_f = m_a \underbrace{\left(1 + \frac{1}{\lambda\left(\frac{A}{F}\right)_s}\right)}_{k} \tag{5.4b}$$

The motivation of the same $c_v = \frac{1}{\gamma-1}\frac{\tilde{R}}{\mathcal{M}}$ for burned and unburned gases is made in two steps. As c_v is coupled to γ and $\mathcal{M}$, the differences in these for burned and unburned gases is interesting. First the ratio of specific heats γ can be approximated to 1.3 for both burned and unburned gases (Heywood, 1988). Second, the molecular weight $\mathcal{M}$ is approximately the same for burned and unburned gases. The difference in molecular weight is approximately 5% (Heywood, 1988) for unburned and burned mixture. Here it will also be assumed that the fresh mixture of air and fuel T_{af} has the same temperature as the air in the intake manifold T_{im}. This is not unreasonable as energy is added to the mixture from heat transfer but energy is also needed to evaporate the fuel (Heywood, 1988).

The ideal gas law now gives the total in-cylinder mass m

$$m = \frac{p_c\left(V_c + V_d\right)}{R_cT_1} \tag{5.5}$$

To determine m the in-cylinder pressure at intake valve closing is needed. As this is not measured it will instead be approximated with the mean intake manifold pressure, that is $p_c = p_{\text{im}}$. The ideal gas also gives the mass of residual gases m_r

$$m_r = \frac{p_{\text{em}}V_r}{R_cT_r} \tag{5.6}$$

The mass of air inside the cylinder during stationary conditions can be derived from Equation (5.1) which results in

$$m_a = \eta_{\text{vol}}\left(N, p_{\text{im}}\right)\frac{p_{\text{im}}V_d}{R_{\text{im}}T_{\text{im}}} + m_\Delta \tag{5.7}$$

Inserting (5.2, 5.4b, 5.5, 5.6, 5.7) into (5.4a) and eliminating c_v gives

$$\frac{p_{\text{im}}\left(V_c + V_d\right)}{R_c} = \eta_{\text{vol}}\left(N, p_{\text{im}}\right)\frac{p_{\text{im}}V_d}{R_{\text{im}}}k + m_\Delta T_{\text{im}}k + \frac{\left(p_{\text{em}_{\text{nom}}} + p_{\text{em}_\Delta}\right)V_r}{R_c} \tag{5.8}$$

The change in exhaust pressure p_{em_Δ} that resulted in the air-mass-offset m_Δ can now be expressed as

$$\frac{p_{\text{im}}\left(V_c + V_d\right)}{R_c} = \eta_{\text{vol}}\left(N, p_{\text{im}}\right)\frac{p_{\text{im}}V_d}{R_{\text{im}}}k + m_\Delta T_{\text{im}}k + \frac{p_{\text{em}\,\text{nom}}V_r}{R_c} + \frac{p_{\text{em}_\Delta}V_r}{R_c} \quad (5.9\text{a})$$

$$\frac{p_{\text{em}_\Delta}V_r}{R_c} = \frac{p_{\text{im}}\left(V_c + V_d\right)}{R_c} - \eta_{\text{vol}}\left(N, p_{\text{im}}\right)\frac{p_{\text{im}}V_d}{R_{\text{im}}}k - m_\Delta T_{\text{im}}k - \frac{p_{\text{em}\,\text{nom}}V_r}{R_c} \quad (5.9\text{b})$$

$$p_{\text{em}_\Delta} = \underbrace{p_{\text{im}}\left(\frac{\left(V_c + V_d\right)}{V_r} - \eta_{\text{vol}}\left(N, p_{\text{im}}\right)\frac{R_c}{R_{\text{im}}}\frac{V_d}{V_r}k\right)}_{\text{When } m_\Delta = 0 \text{ then } p_{\text{em}_\Delta} = 0 \text{ and this term must equal } p_{\text{em}\,\text{nom}}} -$$

$$p_{\text{em}\,\text{nom}} - m_\Delta T_{\text{im}}k\frac{R_c}{V_r} \quad (5.9\text{c})$$

given the volume of the residual gases is V_r. As the term to the left of $p_{\text{em}\,\text{nom}}$ in Equation (5.9c) is linear in p_{im} and changes in p_{im} is small when the exhaust manifold pressure changes, these terms cancel each other which results in:

$$p_{\text{em}_\Delta} = -m_\Delta T_{\text{im}}k\frac{R_c}{V_r} \quad (5.10)$$

In the equations above $k = 1 + \frac{1}{\lambda\left(\frac{A}{F}\right)_s}$ and V_r are constants since the engine runs stoichiometric and does not have variable valve timing. For an ideal otto cycle $V_r = V_c$ but a real engine has valve overlap and heat transfer, therefore V_r is not necessarily equal to V_c.

The resulting exhaust manifold pressure change model, Equation (5.10), has only one parameter and that is $K_e = k\frac{R_c}{V_r}$ which is estimated using the least-square method on measured engine data. In the tested region, from 1800 to 3100 RPM and brake mean effective pressures from 5 to 12 bar, the same $K_e \approx 2.4 \cdot 10^3$ is successfully used.

5.2.3 Summary of Exhaust Pressure Calculation Process

First the air-mass offset m_Δ, Equation (5.1), is calculated. The nominal exhaust pressure is calculated by Equation (5.3) and then inserted into the final Equation (5.10).

$$
\begin{aligned}
m_\Delta\left(W_a, N, p_{\text{im}}, T_{\text{im}}\right) &= W_{\text{at}}\frac{n_r}{N} - \eta_{\text{vol}}\left(N, p_{\text{im}}\right)\frac{p_{\text{im}}V_d}{R_c T_{\text{im}}} \\
p_{\text{em}\,\text{nom}}(W_a) &= p_a + k_1 W_a + k_2 \\
p_{\text{em}}\left(W_a, m_\Delta, T_{\text{im}}\right) &= p_{\text{em}\,\text{nom}}(W_a) - K_e m_\Delta T_{\text{im}}
\end{aligned}
$$

Important second order effects, such as heat transfer, and valve overlap etc. are taken into account by $p_{\text{em}\,\text{nom}}$.

5.3 Validation of Estimator

The estimator is validated using measurements of the exhaust pressure when the wastegate valve is operated manually. An additional exhaust manifold pressure sensor is used for the validation process. In the engine management system, a controller tries to maintain constant air-mass flow through the throttle during the experiments. Since the power to the compressor is reduced when the wastegate is opened the throttle controller will open the throttle to compensate for the lowered air-mass flow. The throttle angle will therefore not be constant during the test, which influences the air-mass flow through the throttle and the air dynamics introduces a small deviation in the estimated air-mass offset m_Δ until the system has reached stationary conditions. Measurement noise and engine pumping fluctuations are reduced by low pass filters on the signals used for the computation of Equation (5.10). Engine pumping fluctuations are also reduced in the measured exhaust manifold pressure by low-pass filters. This validation is performed off-line and all filters used are of zero phase type.

Measurements have been taken for a number of loads at engine speeds between 1800 and 3100 RPM. In each measurement the engine speed is held constant and the wastegate is initially controlled by the ECU. The wastegate is then manually opened and held constant for approximately 10 seconds and then again closed. When the wastegate is opened the exhaust manifold pressure drops as the gases are passed by the turbine. This pressure drop is clearly visible in Figure 5.4, where the pressure drops when the wastegate is opened and rise again when it is closed. During this experiment the air-mass controller maintains a constant air-mass flow through the engine, except for the air transients associated with the sudden changes in wastegate setting.

5.3.1 Stationary Estimated Exhaust Pressure

Stationary validation is performed with and without the air-mass offset information to show the necessity of the additional information. First this is shown in Figure 5.4 where the intake manifold pressure is below ambient and the air-mass flow is controlled to 45 g/s during the experiment.

The controller succeeds in maintaining the desired air-mass flow even for an open wastegate. The nominal exhaust manifold pressure is expressed as a polynomial in air-mass flow and since the air-mass flow is constant the estimated exhaust manifold pressure is also constant. The exhaust manifold pressure drop, caused by the opening of the wastegate, can therefore not be described by this polynomial. When the estimated p_{em_Δ} is applied the drops in exhaust manifold pressure are captured. There are over shoots in the estimated exhaust manifold pressure during transients in the air-mass flow and this is the result of the neglected intake manifold dynamics. It takes a few seconds for the estimated exhaust manifold pressure to converge since stationary conditions have been assumed to calculate the air-mass offset m_Δ. Intake manifold dynamics can be taken into account by using the air-mass-to-cylinder observer described in
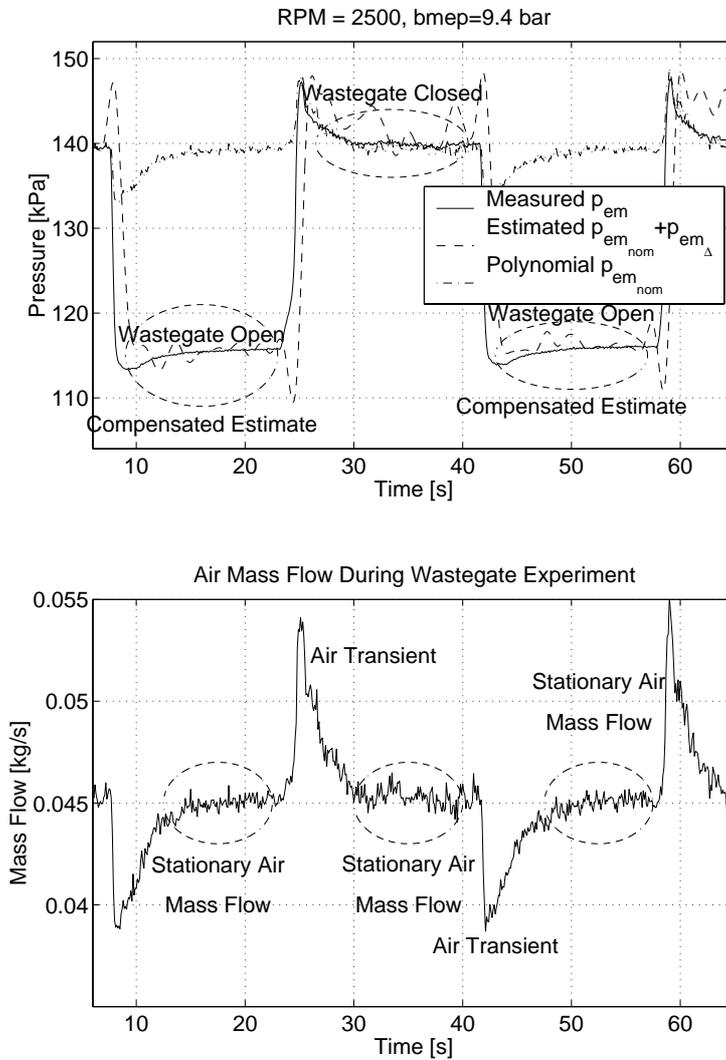
Figure 5.4: *Top:* Measured exhaust manifold pressure data compared to estimated pressure with and without air-mass offset information. The polynomial description gives accurate estimates for nominal wastegate setting, but overestimates the pressure for open wastegate. With the air-mass offset information, Equation (5.10), it is also possible to describe the pressure as the wastegate is open. *Bottom:* When the wastegate is operated there is a short transient in the air-mass flow. Between the transients the air-mass flow is constant, which is marked at stationary flows.

Chapter 4 to calculate m_Δ. The estimated exhaust manifold pressure follows the measured within 4% in Figure 5.4.

More results of applying the method described by Equations (5.1, 5.3, 5.10) are shown in Figure 5.5 (low brake mean effective pressures, bmep) and Figure 5.6 (high bmep) where different settings of the wastegate were used in four different operating points. The wastegate is closed when the exhaust pressure is high and then opened and held there for approximately 10 seconds. What is interesting is that for the lower bmeps in Figure 5.5, approximately 5 bar, the exhaust manifold pressure given by the polynomial do not describe the pressure drops. This is caused by the fact that the intake manifold pressure in these cases are below ambient and the air-mass flow controller manages to supply the engine with constant air-mass flow, which results in constant exhaust manifold pressure unless the p_{em_Δ} component is added. In the bottom plot of Figure 5.5 there is a bias in the estimated exhaust manifold pressure change p_{em_Δ} when the wastegate is closed which is caused by an error in the description of the volumetric efficiency. What is interesting is that the pressure drops approximately 6 kPa when the wastegate opens, which well describes the measured pressure drop. This indicates that even though there is an error in the volumetric efficiency the estimator still gives useful information.

For higher bmeps, Figure 5.6, the pressure in the intake manifold is above ambient and therefore the air-mass-controller does not supply the engine with the same air-mass flow when the wastegate is opened. As the air-mass flow decreases when the wastegate is opened the polynomial description therefore captures the exhaust manifold pressure changes better in this case. When the p_{em_Δ} component is added the estimate is improved significantly.
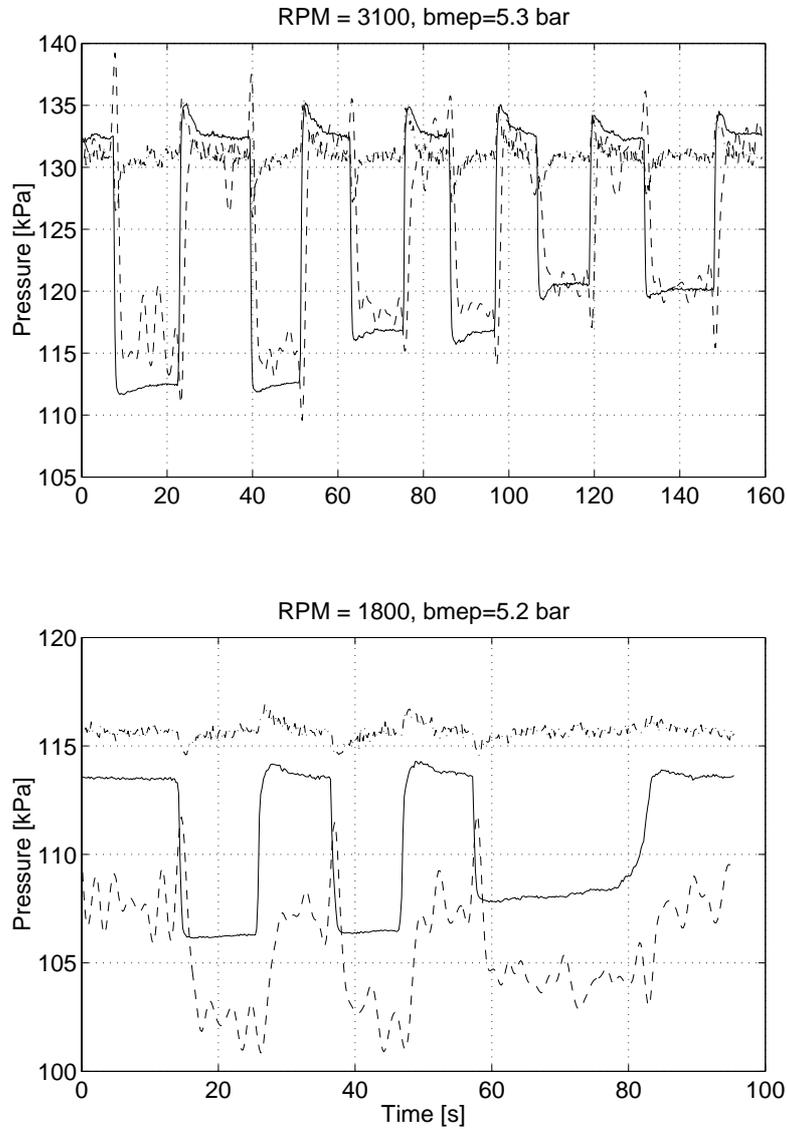
Figure 5.5: Measured exhaust manifold pressure (solid) compared to nominal pressure (dash-dotted), and estimated using the in-cylinder air-mass offset information (dashed). With the additional information the estimates are improved when the wastegate is opened. In the bottom plot there is a stationary offset when the p_{em_Δ} information is added, but the change in exhaust manifold pressure is still described.
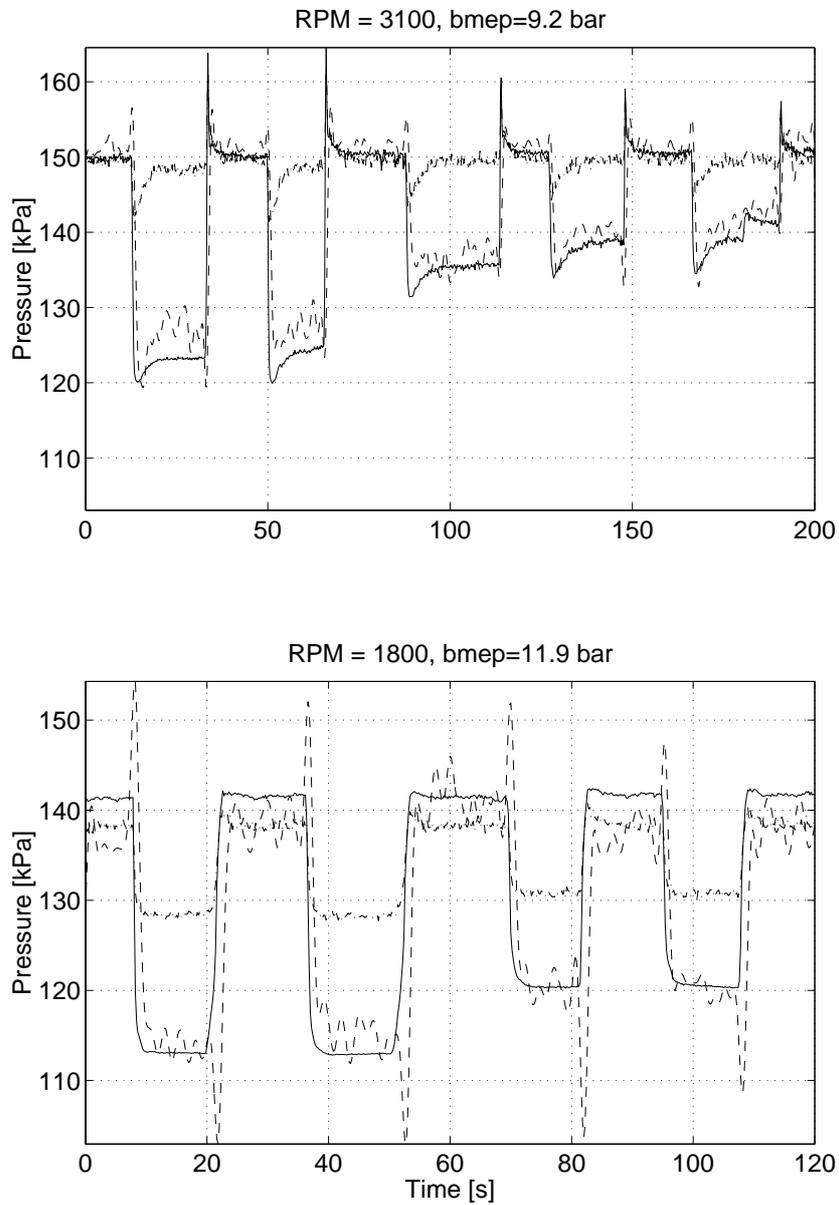
Figure 5.6: Measured exhaust manifold pressure (solid) compared to nominal pressure (dash-dotted), and estimated using the in-cylinder air-mass offset information (dashed). With the additional information the estimates are improved when the wastegate is opened.

5.4   Results

On turbocharged spark-ignition engines with wastegate the absolute exhaust manifold pressure can not be estimated using a simple function of air mass flow. This due to the fact that the exhaust system is made up of four parts: muffler, catalyst, turbine, and wastegate, where the wastegate valve can change position during engine operation and can therefore not be described by a static restriction. For intake manifold pressures below ambient it is possible to achieve the same air mass flow through the engine regardless of wastegate position. Estimates using a static function of air mass flow, W_a, are therefore not suitable for estimating the exhaust manifold pressure particularly at intake manifold pressures below ambient. A non-linear air-to-cylinder model estimates an in-cylinder air-mass-offset m_Δ caused by changes in exhaust manifold pressure. The information m_Δ can then be used together with a description of the nominal exhaust manifold pressure to produce a better estimate of the exhaust manifold pressure. The validation shows that the proposed model based estimator captures the pressure changes well when the wastegate is opened and closed.

To estimate the exhaust manifold pressure, only sensors on the intake side are used. Good estimates are produced provided that there is an accurate description of the volumetric efficiency. In the estimation of the exhaust manifold pressure offset p_{em_Δ}, given that the engine is running stoichiometricly, there is only one parameter that influences the estimate and that is the residual gas volume V_r. The estimated pressure can be used in a diagnosis system, e.g. to check the back pressure caused by the exhaust system.

6

Exhaust Manifold Leakage Detection — A Feasibility Study

The three way catalyst (TWC) reduces most of the emissions from modern spark ignited (SI) engines when it is operated with a stoichiometric air/fuel ratio as input (Heywood, 1988; Degobert, 1995). A leak in the exhaust system before the catalyst increases emissions for two reasons: First, untreated gases leak out. Second, due to waves in the exhaust system (D.E. Winterbone, 1999), oxygen can leak into the exhaust manifold and influence the measured λ. The two cases are shown in Figure 6.1 where the exhaust manifold pressure is sampled with a high frequency for two different engine loads. In the lower plot the minimum pressure is above ambient all the time which results in a continuous leakage of gases out of the exhaust manifold. The second case is shown in the top plot where the minimum pressure is below ambient pressure during approximately a quarter of the period. If there is a hole present in this case oxygen would leak in and mix with the exhaust gases. The oxygen would also be transported away from the hole by the velocity of the gas. Gases leaking out of the hole is therefore not necessarily the same as the gases leaking in.

In the engine control system there is a closed loop air/fuel ratio PI-controller, with feed-back from the binary oxygen sensor. If oxygen leaks into the exhaust manifold it may cause a bias in the integrating part or an wind up of the controller. The additional oxygen entering the exhaust manifold makes the engine run rich when it reaches the oxygen sensor. Running the engine rich increases fuel consumption and the emissions of hydrocarbons, carbon monoxide and dioxide. With the rear oxygen sensor after the catalyst the engine control system can compensate for the excess air.

Leakages in the exhaust will increase the emissions and it is therefore de-
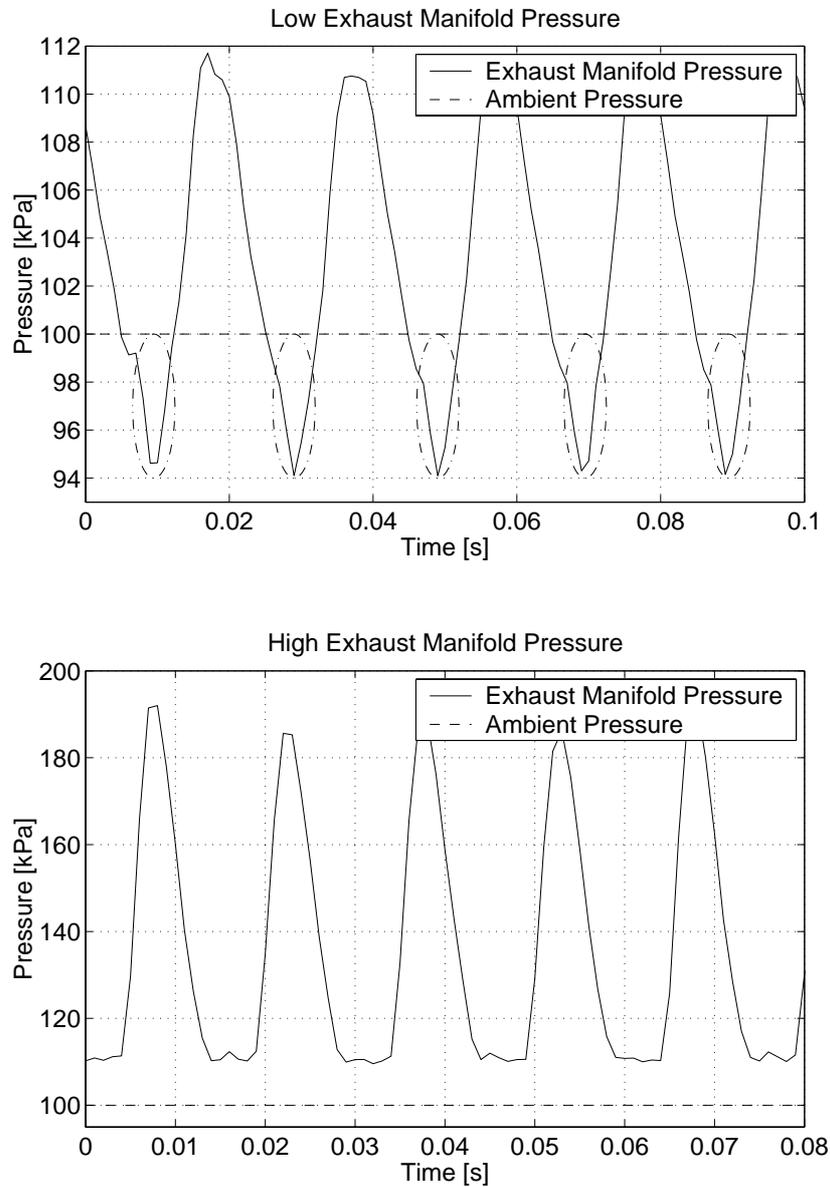
Figure 6.1: Cyclic exhaust pressure variations during the stationary operation. *Top:* Low pressures are referred to exhaust manifold pressure where the pressure reaches values below ambient. In the figure these are marked with ellipses. When the pressure is below ambient, oxygen may leak into the exhaust manifold. *Bottom:* All of the pressure wave is above ambient pressure and this case is referred to as high pressure. Here exhaust gases leaks out continuously.

sirable to detect them. Examples of current methods, used at service stations, for detecting leakages in the exhaust are: listening to the engine sound, or filling the exhaust with smoke injected via the tail pipe and looking for presence of smoke in the engine compartment. Here a computerized method to detect leakages in the exhaust manifold is proposed.

The basis for the method is that oxygen leaks in at low exhaust manifold pressures and this changes the in-cylinder air/fuel. At higher loads the continuous flow of gases out of the exhaust lowers the exhaust manifold pressure. The exhaust manifold pressure is normally not measured but it can be estimated, using the method presented in Chapter 5.

The feasibility of a diagnosis system for detecting exhaust manifold leaks is studied. The proposed method is based on estimated air/fuel ratio and estimated exhaust manifold pressure drop. The diagnosis method is supported by measurements of leakages on a turbo charged SAAB SI production engine with wastegate. The sensors used are: binary oxygen sensor(s), intake manifold pressure and temperature sensors, and the air mass flow sensor. One actuator signal is also used, the injection time signal.

6.1 Analysis of the Impact of a Leakage

For the case of emissions leaking out, an approximation is made to estimate the diameter required to exceed emission levels for EURO-3 and 4. In Figure 6.2 a schematic of the exhaust system is shown with TWC and a possible leakage before the TWC. In the exhaust system the mass of specie i is m_i, and through the hole a fraction y_L leaks out. Now given that the maximum allowed emission mass of species i after the TWC is lim_i and the conversion efficiency of the TWC for species i is η_i. For the exhaust emission regulations to be fulfilled the following inequality must hold $m_i (1 - \eta_i) \leq lim_i$. The maximum mass fraction y_L that can leak out is then given by the following inequality

$$y_L \leq \left(\frac{lim_i}{m_i} - 1 \right) \frac{1}{\eta_i} + 1$$

To give an upper bound of the leakage fraction y_L all emissions are assumed to originate from the leak. This corresponds to setting the efficiency of the TWC η_i to one. This results in

$$y_L \leq \frac{lim_i}{m_i} \tag{6.1}$$

To estimate m_i a simulation of the EURO-3 driving cycle is performed using a longitudinal vehicle model of a SAAB 9[5]. The model estimates the mean exhaust manifold pressure in the cycle and approximates the emissions before the TWC. Emissions are approximated using static models of exhaust gas composition as a function of λ. Using this simplified raw emissions estimation process, the resulting emissions before the TWC are $m_{CO} \approx 14$ g/km, $m_{HC} \approx 2.6$ g/km,

and $m_{NO_x} \approx 1$ g/km. The maximum allowed emissions for EURO-3 and EURO-4 are listed in Table 6.1.

	EURO-3	EURO-4
Specie	Maximum mass	Maximum mass
CO	$lim_{CO} = 2.3$ g/km	$lim_{CO} = 1.0$ g/km
HC	$lim_{HC} = 0.2$ g/km	$lim_{HC} = 0.1$ g/km
NO_x	$lim_{NO_x} = 0.15$ g/km	$lim_{NO_x} = 0.08$ g/km

Table 6.1: Emission levels for EURO-3 and EURO-4

Now an estimation of m_i exists and also the limits lim_i are known which means that y_L can be estimated using Equation (6.1). Given y_L the mass of specie i that leaks out is $m_i y_L$ and it can also be estimated by assuming the flow out of the leak. Given the mean exhaust manifold pressure the mass flow through the leak is assumed to be a compressible flow through a restriction with diameter d. The compressible flow through the restriction is given in Equation (4.5a) and it is used with the following exceptions: $p_r = \frac{p_a}{p_{em}}$, $\gamma = 1.3$, and $A_{\text{eff}} = \pi \frac{d^2}{4}$. With these assumptions the emission levels for EURO-3 is exceeded by leakage out of a 6 mm hole and EURO-4 by a 4 mm leak.
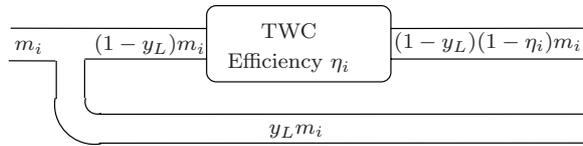
Figure 6.2: The engine produces the mass m_i of specie i, where i can be e.g. carbon monoxides. The mass fraction that passes through the leak is y_L and the conversion efficiency of the TWC for specie i is η_i.

6.2 Definition of Low and High Exhaust Pressure

The proposed diagnosis method is based on a partition of exhaust pressures into low and high pressures, see Figure 6.1. The first case occurs when the minimum of the exhaust pressure waves are below ambient. If a leak is present here air may leak in. Hence *low pressure* will be used in the text to refer to operating points where the pressure in the exhaust manifold is below ambient for parts of the time. This condition is shown in the top of Figure 6.1.

High pressure appears when the lowest pressure is higher than the ambient pressure all the time, which is the case in the lower plot of Figure 6.1. A leak

in this case will cause emissions to leak out all the time and there is a drop in exhaust manifold pressure compared to the fault free case.

6.2.1 Using Air Mass Flow to Partition Exhaust Pressure

Low pressures are defined from measurements as where the minimum of the exhaust manifold pressure wave is below 98 kPa and high pressures are defined for minimum pressures above 102 kPa. The limits are here chosen around ambient pressure which is approximately 100 ± 2 kPa. As the exhaust manifold pressure is not normally measured, another method has to be used. In (Eriksson et al., 2001) the mean exhaust back pressure is described as almost linear in mass flow through the engine, which is also seen in Figure 5.3. The air-mass flow will consequently be used to partition the data in low and high pressure.

The result of the partition is shown in Figure 6.3. For air mass flows under 25 g/s the lowest exhaust manifold pressure is below 98 kPa and for air mass flows above 32.5 g/s the minimum exhaust manifold pressure is over 102 kPa. Flows in between theses limits are not categorized as low or high using this method, but this categorization captures the majority of the operating conditions.

6.3 Proposed Design of the Diagnosis System

Now the effects of a leakage in different operating conditions have been investigated. To build a diagnosis system that can detect leakages the statements of the system is decided first:

Abbreviation	Explanation
NF	No fault = No Leak
EML	Exhaust Manifold Leakage

Several diagnosis methods (Gertler, 1991; Nyberg, 1999) tests measured data against fault models and the statement is the fault corresponding to the model that best explains the measured data. In this case fault models are developed for the fault free case (NF) and for the exhaust manifold leakage case (EML).

When the models of the faults are fixed, test statistics are developed for the fault model. A test statistic is a function of the sampled data (Casella and Berger, 1990), like the mean value or standard deviation of the data.

Initially the fault models are described in words for the two statements. As the system behaves differently depending on exhaust manifold pressure there are two cases for each fault model: one for low pressures, where air can leak into the exhaust manifold, and the other case is for high pressures where exhaust gases continuously leaks out.
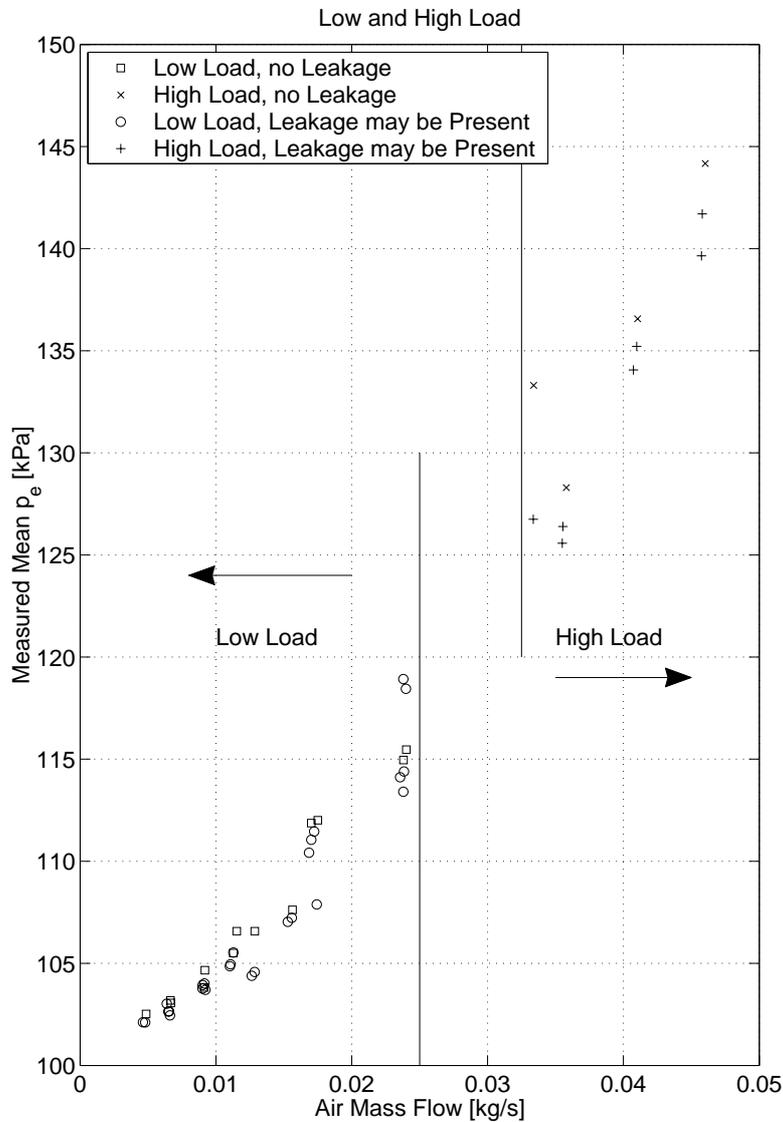
Figure 6.3: Mean exhaust manifold pressure plotted against air mass flow for low and high exhaust manifold pressures. There is a distinct border between the selected limits for high and low load, which is shown as vertical lines in the plot above. For low loads the lowest exhaust manifold pressure is below 98 kPa and for high loads the lowest pressure is above 102 kPa. Measurements with leakages are included for high pressures as the exhaust manifold pressure without leak would be higher and for low pressures as even with the leakage present the minimum pressure drops below 98 kPa.

For the *No Fault (NF)* case the exhaust manifold is assumed to be leak free and this means that there is no additional oxygen present for low exhaust pressures. At higher exhaust pressures the pressure does not differ from the nominal pressure, that is no additional pressure drop.

When there is an *Exhaust Manifold Leakage (EML)* present there are additional oxygen in the exhaust manifold at low exhaust pressures. For higher pressures there is an increased mass flow out of the manifold which causes the exhaust manifold pressure to drop compared to nominal exhaust manifold pressure.

6.3.1 Fault Models

The fault models need knowledge of oxygen in the exhaust manifold and of exhaust manifold pressure drop. Therefore models of oxygen content and exhaust manifold pressure are developed. To develop the models some assumptions are necessary. As the TWC does not work for a cold engine, and the engine models are only valid for a warmed up engine, so a warmed up engine will be required. Finally the engine is assumed to run at a steady-state, that is the same speed and load is held constant. In the experiments made here, the engine have been run in the same state for approximately 20 seconds. The measured data is time discrete and the samples are assumed to be independent. First the oxygen content model is described. In the nomenclature in Section A.1 there is a description of the symbols used.

Oxygen Content Model

The lambda sensor is sensitive to oxygen in the exhaust gases and the lambda-controller has at least one integration part which stores information of the air/fuel ratio. As the objective of the controller is to maintain stoichiometric conditions at the oxygen sensor, and when air leaks into the exhaust manifold the oxygen sensor is disturbed. This results in that the air/fuel ratio on the intake side will be rich, $\lambda < 1$. The intake port air/fuel ratio can be estimated using measured the air-mass flow W_{a} and injection time t_{inj} together with a model of the injector. The current air/fuel ratio, called λ_{est}, can now be estimated given the fuel-specific stoichiometric air/fuel ratio $\left(\frac{A}{F}\right)_s$ is known

$$\lambda_{\mathrm{est}}(W_{\mathrm{a}}, t_{\mathrm{inj}}) = \frac{W_{\mathrm{a}}}{\left(\frac{A}{F}\right)_s \underbrace{K_{\mathrm{inj}}\left(t_{\mathrm{inj}} - t_0\right)}_{\text{Injector model}} \frac{N}{n_r}} \tag{6.2}$$

One major advantage is that the air/fuel $\lambda_{\mathrm{est}}(W_{\mathrm{a}}, t_{\mathrm{inj}})$ ratio still can be calculated regardless of how the front and rear feed-back from the oxygen sensors influences the controller. This means that no information of how the controllers are implemented is necessary. A disadvantage is that there are three parameters $\left(\frac{A}{F}\right)_s$, K_{inj}, and t_0. Model errors in the injection constant K_{inj} has the same

impact as errors in the stoichiometric air/fuel ratio $\left(\frac{A}{F}\right)_s$. Errors in the needle lift time t_0 are most evident for small injection times which is the case for low exhaust pressures where the air mass flow is low.

Exhaust Pressure Drop Model

For higher mass flows the minimum exhaust pressure is above the atmospheric pressure and therefore exhaust gases will leak out continuously. This constant leak will decrease the mean value of the exhaust manifold pressure, which is shown in Figure 6.4. In the fault free case the mean exhaust manifold pressure is 144 kPa, but when a 4 mm leak is present the pressure drops to 141.7 kPa and for the 5 mm leak the pressure drops down to 139.7 kPa. This is a clear indication that there is an exhaust manifold pressure drop for leakages at high pressures.

Unfortunately the absolute exhaust manifold pressure is not measured on production SI-engines. However the information on the exhaust manifold pressure is present in the intake system, which is shown in Chapter 5.

The derivation of exhaust manifold pressure using sensors on the intake side is briefly summarized as follows. Calculate whether the cylinder is filled with the expected mass of air. If not the offset m_Δ will differ from zero, see Equation (5.1). Since the air-mass-offset m_Δ is influenced by the exhaust manifold pressure a corresponding change in exhaust manifold pressure p_{em_Δ}, from nominal in Equation (5.3), can be estimated, Equation (5.10). The equations needed to estimate the exhaust manifold pressure given information in the intake manifold can be summarized as

$$m_\Delta\left(W_{\mathrm{a}}, N, p_{\mathrm{im}}, T_{\mathrm{im}}\right) \;=\; W_{\mathrm{at}}\frac{n_r}{N} - \eta_{\mathrm{vol}}\left(N, p_{\mathrm{im}}\right)\frac{p_{\mathrm{im}}V_d}{R_{\mathrm{c}}T_{\mathrm{im}}} \tag{6.3}$$

$$p_{\mathrm{em}_{\mathrm{nom}}}(W_{\mathrm{a}}) \;=\; p_{\mathrm{a}} + k_1 W_{\mathrm{a}} + k_2 \tag{6.4}$$

$$p_{\mathrm{em}_\Delta}\left(m_\Delta, T_{\mathrm{im}}\right) \;=\; -K_e m_\Delta T_{\mathrm{im}} \tag{6.5}$$

In Equation (5.10) K_e is a constant which is identified using a least square technique.

6.4 A Preliminary Feasibility Study of the Concept

For low pressures the oxygen content is monitored in form of the mean of λ_{est}, denoted $\overline{\lambda_{\mathrm{est}}}$. When a leak is present $\overline{\lambda_{\mathrm{est}}} < 1$, which indicates that the engine is running rich. At high pressures the exhaust manifold pressure would be desirable but as it is not normally measured the mean value of the exhaust manifold pressure drop p_{em_Δ}, denoted $\overline{p_{\mathrm{em}_\Delta}}$, is used instead. A drop in exhaust manifold pressure, that is $\overline{p_{\mathrm{em}_\Delta}} < 0$, indicates a leakage. Two test statistics are therefore proposed: for low pressures the estimated air/fuel ratio $\overline{\lambda_{\mathrm{est}}}$ and for high pressures the exhaust manifold pressure drop $\overline{p_{\mathrm{em}_\Delta}}$.
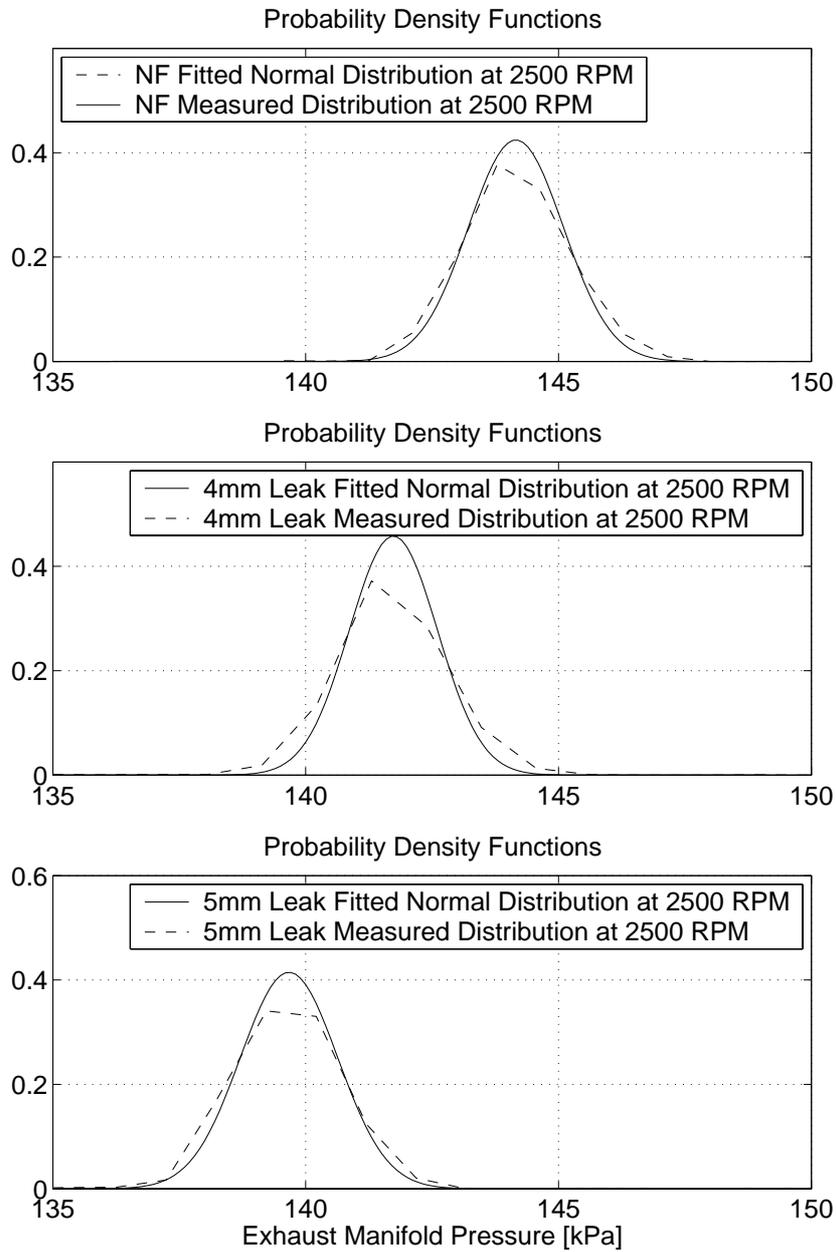
Figure 6.4: Measurements at a high exhaust pressure at 2500 RPM and an air mass flow of 46 g/s. When a leak is present the mean value of the exhaust manifold pressure drops, that is the centers of the density function tends to the left.

Both test statistics are modeled as constant parameters μ_x and each parameter is estimated from a measured signal $y(t)$, that in this case is λ_{est} or p_{em_Δ}. The measured signal is subjected to noise $v(t)$ originating from measurements and model errors. The noise is assumed to have a normal distribution $N(0, \sigma_v)$ and to be independent. In top of Figure 6.5 the assumption of normal distributed noise is supported for λ_{est}, as the normal distribution fits the measured distribution very well. For estimated exhaust manifold pressure drop distribution the fit is also good, Figure 6.6, but not as good as for λ_{est} since less data is available here.

Now to use the test statistics there are several methods to select thresholds to which the test statistic is tested against. Several methods to design such tests have been proposed, e.g. in (Nyberg, 1999). In this study there are to little knowledge of the distributions in the exhaust manifold leakage case to perform a threshold selection. The selection of the threshold is a compromise between giving false alarms (too low threshold) and to miss detections (too high threshold).

Here only the distributions of the test statistics is calculated for a general test statistic μ_x which is calculated from independent time discrete measurements $y(i)$, which are subjected to noise $v(i) \sim N(0, \sigma_v)$. The test statistic is the mean value of the measured signal $y(i)$ and it is called $\hat{\mu}_x$

$$\hat{\mu}_x = \frac{1}{N}\sum_{i=1}^{N} y_i = \mu_x + \frac{1}{N}\sum_{i=1}^{N} v_i \sim N(\mu_x, \frac{1}{\sqrt{N}}\sigma_v) \tag{6.6}$$

The standard deviation of the estimate $\hat{\mu}_x$ is $\sigma_{\hat{\mu}_x} = \frac{\sigma_v}{\sqrt{N}}$ which depends on the number of samples N.

6.4.1   Low Exhaust Pressures

Here the estimate of oxygen content is modeled using the mean value of sampled λ_{est} as a test statistic

$$\overline{\lambda_{\mathrm{est}}} = \frac{1}{N}\sum_{i=1}^{N} \lambda_{\mathrm{est}}(W_{\mathrm{a}}, t_{\mathrm{inj}})(i) \tag{6.7}$$

In Figure 6.5 the distributions of a fault free case is shown together with three leakages at low exhaust pressures. In the fault free case λ_{est} is distributed around stoichiometric. On the other hand, when a leak is present λ_{est} tends to the left which means that the engine is running rich. In the NF case $\overline{\lambda_{\mathrm{est}}}$ is one and when a leak is present it is less than one. This is a good indication of that the mean value of the calculated air/fuel ratio is a good test statistic.
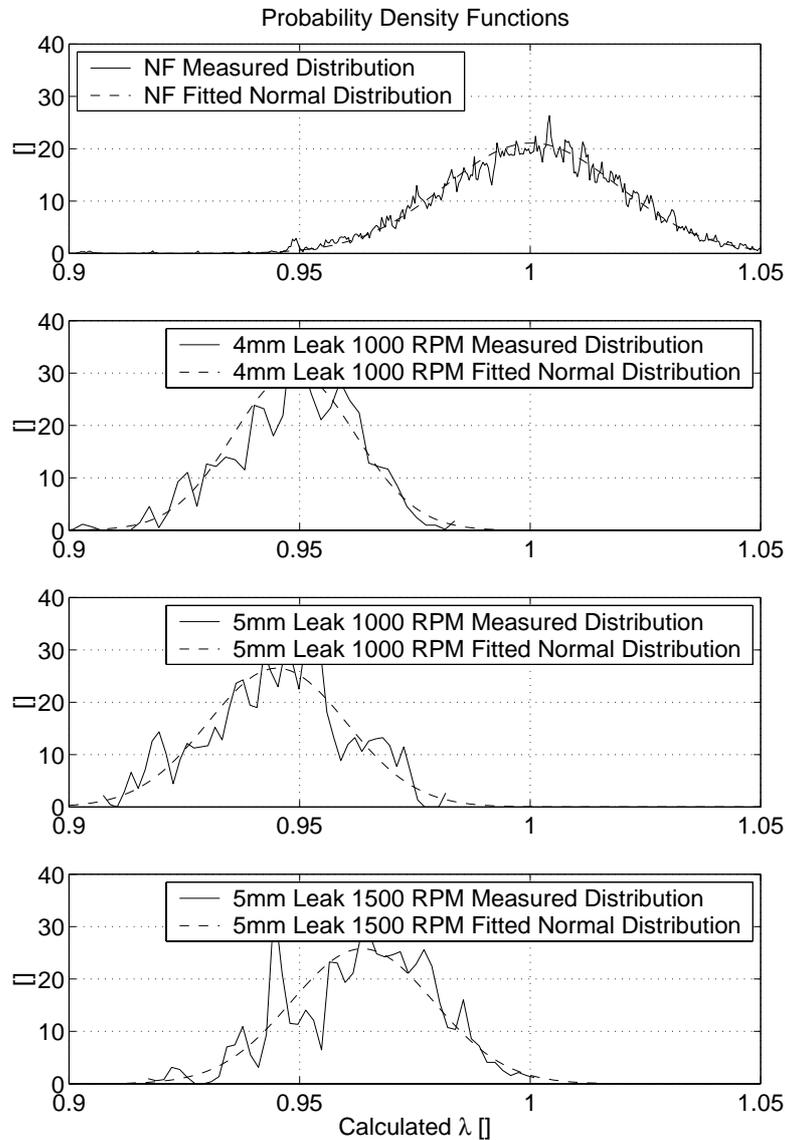
Figure 6.5: Measurements taken at 1000 RPM and an air mass flow of 0.5 g/s. In the measurement at 1500 RPM the air mass flow is 0.64 g/s. In the no fault case the estimated λ_{est} is around stoichiometric. When a fault is present the mean value, the center of the function, tends to the left. This is the case when there is a 4mm and a 5 mm leak. For the NF case there is considerably more measurement data than for the leakage cases.
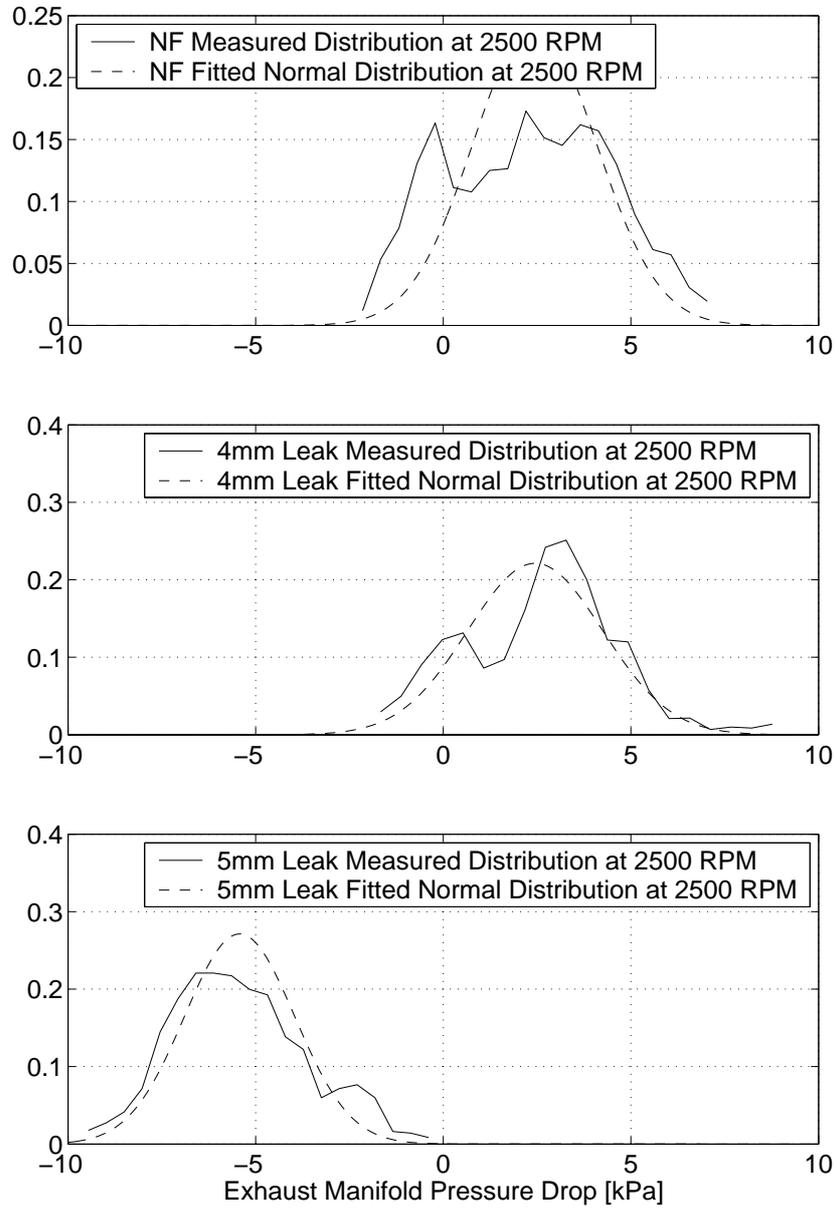
Figure 6.6: Here the same measurements as in Figure 6.4 is used, but the estimated pressure difference p_{em_Δ} is shown instead. When a fault is present the mean value, centers of the density function, tends to the left. In the middle plot the p_{em_Δ} should move a bit to the left to comply with the center of Figure 6.4.

6.4.2 High Exhaust Pressures

In Figure 6.4 measured exhaust manifold pressure is shown with and without a leak for the same speed and load. When a leak is present the exhaust manifold pressure drops, which supports the use of exhaust manifold pressure drop as a test statistic for high exhaust pressures. As p_{em} is normally not measured, estimates of changes in exhaust manifold pressure from nominal pressure is used instead. These are made available made by the virtual exhaust manifold pressure sensor p_{em_Δ}. In Figure 6.6 the distribution of the estimated exhaust manifold pressure difference (p_{em_Δ}) is shown.

$$\overline{p_{em_\Delta}} = \frac{1}{N} \sum_{i=1}^{N} p_{em_\Delta}(m_\Delta, T_{im})(i) \tag{6.8}$$

6.4.3 Future Work

More measurements are needed to get more knowledge of the data distributions in the exhaust manifold leakage case for both λ_{est} and p_{em_Δ}. For the exhaust manifold pressure drop more data is also needed in the fault free case as less data is available here than for $\overline{\lambda_{est}}$. Then research is needed to select number of data that should be used to calculate test statistics $\overline{\lambda_{est}}$ and $\overline{p_{em_\Delta}}$. Then thresholds for the test statistics can be decided based on a compromise using the knowledge of the statistical distributions.

6.5 Current Status

A promising diagnosis method for detecting leakages in the exhaust manifold has been presented. It uses the estimated air/fuel ratio and a mean value model of the exhaust manifold pressure. The first results are encouraging but the experiments are not conclusive yet.

For low exhaust manifold pressures, the oxygen content of the exhaust gases is monitored. When a leak is present air leaks into the exhaust manifold, mixes with the exhaust gases and is transported away from the leak. An increase in oxygen therefore indicates a leakage. The method is sensitive to fuel changes as it estimates the current air/fuel ratio, but it is independent of the implementation of the air/fuel controller and feed-back from a rear oxygen sensor.

At high exhaust manifold pressures, there is a continuous flow out of the exhaust manifold causing the pressure to drop, which can be detected using a virtual exhaust manifold pressure sensor. Exhaust manifold pressure estimation relies on accurate sensors on the intake side together with an good description of the volumetric efficiency. No additional sensors in the exhaust manifold are necessary.

7

CONCLUSIONS

Turbocharged spark-ignited (SI) engines are getting more popular as they provide good fuel economy and high power output. They are commonly equipped with a wastegate that influences the back pressure and air-mass flow to the cylinders. These quantities influence the performance but they are normally not measured, and therefore they have to be estimated using available sensors in the intake manifold.

Air-mass to cylinder estimation is performed using speed-density methods, and the focus is on stationary mass-balance in the intake manifold for changes in the wastegate setting. A new 2-state air-mass to cylinder observer, with feedback from measured intake manifold pressure, is proposed by combining the strengths of two studied observers from the literature. The states of the proposed observer are intake manifold pressure and an in-cylinder air-mass offset. The air-mass offset describes the change in air-mass in the cylinder compared to what is expected through the mapped volumetric efficiency. Together with the proposed observer a method to tune it is also suggested. The contribution is the air-mass to cylinder observer which achieves stationary mass-balance and estimates the same intake manifold pressure as the measured.

A major contribution of this thesis is an exhaust manifold pressure estimator, which is based on the in-cylinder air-mass offset information from the suggested 2-state air-mass to cylinder observer. The estimation relies on a simplified gas exchange process and energy conservation. Given the sensor information on the intake side, and a description of a nominal exhaust manifold pressure, only one additional parameter is necessary to describe the change in exhaust manifold pressure introduced by the wastegate. The estimator describes the changes in

exhaust manifold pressure well for different settings of the wastegate.

The last contribution is a proposal for a method to detect leakages in the exhaust manifold before the first oxygen sensor. When a leak is present there is either oxygen leaking into the exhaust manifold that disturbs the air/fuel ratio controller, or the leakage flow causes a drop in exhaust manifold pressure. If the air/fuel ratio controller is disturbed this can be detected by estimating the air/fuel ratio using measured air-mass flow and injected fuel. If the leak causes an exhaust manifold pressure drop, this can be detected using the exhaust manifold pressure estimator. More measurements and research is needed to fully develop the method, but the first results are encouraging.

To conclude, the result of changes in exhaust manifold pressure conditions have been investigated. Given only the information from the sensors on the intake side successful estimates of changes in air-mass to cylinders caused by a changed setting of the wastegate and successful estimates the exhaust manifold pressure have been performed.

References

Per Andersson and Lars Eriksson. Air-to-cylinder observer on a turbocharged si-engine with wastegate. In *Electronic Engine Controls*, number SAE Technical Paper 2001-01-0262 in SP-1585, pages 33–40. SAE 2001 World Congress, March 2001, Detroit, MI, USA, March 2001a.

Per Andersson and Lars Eriksson. Exhaust manifold pressure estimation on a turbocharged SI-engine with wastegate. In *IFAC Workshop - Advances in Automotive Control; Karlsruhe, Germany*, pages 395–400, March 2001b.

Per Andersson and Lars Eriksson. Detection of exhaust manifold leaks on a turbocharged si-engine with wastegate. In *Electronic Engine Controls*, number SAE Technical Paper 2002-01-0844 in SP-1704, 2002.

I. Arsie, F. De Franceschi, C. Pianese, and G. Rizzo. O.d.e.c.s. - a computer code for the optimal design of s.i. engine control strategie. Number SAE Technical Paper No. 960359 in SP-1168, pages 195–207, 1996.

Johan Bergström and Jan Brugård. Modeling of a turbo charged spark ignited engine. Master's thesis, Linköping, 1999. URL http://www.fs.isy.liu.se/Publications/. LiTH-ISY-EX-2081.

G. Casella and R. L. Berger. *Statistical Inference*. Duxbury Press, 1990.

Chen-Fang Chang, Nicholas P. Fekete, and J. David Powell. Engine air-fuel ratio control using an event-based observer. Number SAE Technical Paper 930766, 1993.

Alain Chevalier, Christian Winge Vigild, and Elbert Hendricks. Predicting the port air mass flow of SI engines in air/fuel ratio control applications. In *Electronic Engine Controls*, number SAE Technical Paper 2000-01-0260 in SP-1500, 2000.

R.J. Pearson D.E. Winterbone. *Design Techniques for Engine Manifolds Wave Action Methods for IC Engines*. SAE International, 1999. ISBN 0-7680-0482-9.

P. Degobert. *Automobiles and Pollution*. Society of Auotomotive Engineers, Inc., 1995. ISBN 1-56091-563-3.

Lars Eriksson, Simon Frei, Christopher Onder, and Lino Guzzella. Control and optimization of turbo charged spark ignited engines. Submitted to IFAC world congress, Barcelona, Spain, 2002.

Lars Eriksson, Lars Nielsen, Jan Brugård, Johan Bergström, Fredrik Pettersson, and Per Andersson. Modeling of a turbocharged spark ignited engine with waste gate. In *IFAC Workshop - Advances in Automotive Control; Karlsruhe, Germany*, pages 379–388, March 2001.

N.P Fekete, U. Nester, I. Gruden, and J.D. Powell. Model-based air-fuel ratio control of a lean multi-cylinder engine. Number SAE Technical Paper 950846, 1995.

J. Gertler. Analytical redundancy methods in fault detection and isolation; survey and synthesis. In *IFAC Fault Detection, Supervision and Safety for Technical Processes*, pages 9–21, Baden-Baden, Germany, 1991.

L. Guzzella, U. Wenger, and R. Martin. Ic-engine downsizing and pressure-wave supercharging for fuel economy. Number SAE Technical Paper No. 2000-01-1019, 2000.

Heinz Heisler. *Advanced engine technology*. Arnold, Hodder Headline Group, 1997. ISBN 1-56091-734-2.

E. Hendricks and S. C. Sorensen. Mean value modelling of spark ignition engines. 1990. SAE Technical Paper 900616.

E. Hendricks, T. Vesterholm, and S. C. Sorensen. Nonlinear, closed loop, SI engine control observers. 1992. SAE 920237.

John B. Heywood. *Internal Combustion Engine Fundamentals*. McGraw-Hill International Editions, 1988.

Mrdjan Jankovic and Steve W. Magner. Air-charge estimation and prediction in spark ignition internal combustion engines. In *Proceedings of the American Control Conference*, pages 217–221, San Diego, California, June 1999.

Per B. Jensen, Mads B. Olsen, Jannik Poulsen, Elbert Hendricks, Michael Fons, and Christan Jepsen. A new family of nonlinear observers for SI engine air/fuel ratio control. In *Electronic Engine Controls*, number SAE Technical Paper 970615 in SP-1236, pages 91–102, 1997.

Allan J. Kotwick, John D. Russell, Ross Pursifull, and Don Lewis. An air meter based cylinder air charge estimator. In *Electronic Engine Controls 1999*, number SAE Technical Paper 1999-01-0856 in SP-1419, pages 81–90, 1999.

Mattias Krysander. Luftflödet förbi en trottel. Master's thesis, Linköping University, SE-581 83 Linköping, 2000. URL `http://www.fs.isy.liu.se/Publications/`.

Peter J. Maloney and Peter M. Olin. Pneumatic and thermal state estimators for production engine control and diagnostics. In *Diagnostics and Control*, number 980517 in SP-1357, pages 53–64, 1998.

Martin Müller, Elbert Hendricks, and Spencer C. Sorenson. Mean value modelling of turbocharged spark ignition engines. In *Modeling of SI and Diesel Engines*, number SAE Technical Paper 980784 in SP-1330, 1998.

Mattias Nyberg. *Model Based Fault Diagnosis: Methods, Theory, and Automotive Engine Applications*. PhD thesis, Linköping University, June 1999.

Mattias Nyberg and Lars Nielsen. Model based diagnosis for the air intake system of the SI-engine. Number SAE Technical Paper 970209, 1997.

Fredrik Pettersson. Simulation of a turbo charged spark ignited engine. Master's thesis, Linköping University, SE-581 83 Linköping, 2000. URL `http://www.fs.isy.liu.se/Publications/`.

Michael G. Safanov and Michael Athans. Robustness and computational aspects of nonlinear stochastic estimators and regulators. *IEEE Transactions on Automatic Control*, AC-23(4):717–725, August 1978.

Yaojung Shio and John J. Moskwa. Model-based cylinder-by-cylinder air-fuel ratio control for SI engines using sliding observers. In *Proceedings of the 1996 IEEE International Conference on Control Applications*, pages 347–354, Dearborne, MI, September 1996.

Charles Fayette Taylor. *The Internal-Combustion Engine in Theory and Practice*, volume 1. The M.I.T. Press, 2 edition, 1994.

Tung-Cing Tseng and Wai K. Cheng. An adaptive air/fuel ratio controller for SI engine throttle transients. In *Electronic Engine Controls 1999 (SP-1419)*, number SAE Technical Paper 1999-01-0552, pages 37–48, 1999.

N. Watson and M.S. Janota. *Turbocharging the Internal Combustion Engine*. The Macmillan Press Ltd, 1982. ISBN 0-333-24290-4.

A

Appendix

A.1 Nomenclature

Symbol	Description
$A\left(\alpha\right)$	Throttle area
$A_{\text{eff}}\left(\alpha\right)$	A fitted function to the measured product of area and discharge coefficient
$\left(\frac{A}{F}\right)_s$	Stoichiometric air/fuel ratio
$C_d\left(\alpha\right)$	Discharge coefficient for the throttle
c_v	Specific heat at constant volume
k_1	Constant in polynomial for nominal exhaust manifold pressure
k_2	Constant in polynomial for nominal exhaust manifold pressure
k	Scaling factor to calculate air and fuel mass given air mass, $k = 1 + \frac{1}{\lambda\left(\frac{A}{F}\right)_s}$
K_e	Constant in equation for exhaust manifold pressure difference
K_{im}	Filling/emptying constant $K_{\text{im}} = \frac{R_{\text{im}}T_{\text{im}}}{V_{\text{im}}}$ for the intake manifold
K_{inj}	Maximum delivered fuel mass per second
K_{obs}	Feed-back gain from pressure estimation error in observer using proportional feed-back to the $\hat{p}_{\text{im}}$ state

continued from previous page	
Symbol	**Description**
K_1	Feed-back gain from pressure estimation error in the 2-state observer to the $\hat{p}_{\mathrm{im}}$ state
K_2	Feed-back gain from pressure estimation error in the 2-state observer to the $\hat{m}_\Delta$ state
lim_i	Maximum allowed emission mass of specie i
L_1	Time constant in (Tseng and Cheng, 1999)
$\mathcal{M}$	Molar mass
$\mathcal{M}_a$	Molar mass of air
$\mathcal{M}_f$	Molar mass of fuel
m	In-cylinder mass at inlet valve closing
m_a	Mass of air the cylinder
m_f	Mass of fuel the cylinder
m_i	Mass of untreated emission of specie i
m_r	Residual gas mass
m_Δ	In-cylinder air-mass offset
$\hat{m}_\Delta$	Estimated in-cylinder air-mass offset
n_r	Number of revolutions per cycle
N	Engine speed i revolutions per second. In Chapter 6 this also denotes the number of samples
$\tilde{R}$	Gas constant, 8.31 $[\frac{J}{\mathrm{mole}\cdot K}]$
p_a	Ambient pressure
p_c	In-cylinder pressure at intake valve closing
p_{em}	Exhaust manifold pressure
$p_{\mathrm{em_{nom}}}$	Nominal exhaust manifold pressure
p_{em_Δ}	Exhaust manifold pressure difference from nominal pressure
$\overline{p_{\mathrm{em}_\Delta}}$	Mean of exhaust manifold pressure difference from nominal pressure
p_{ic}	Pressure between intercooler and throttle
p_{im}	Intake manifold pressure
$\hat{p}_{\mathrm{im}}$	Estimated intake manifold pressure
p_r	Pressure ratio $p_r = \frac{p_{\mathrm{im}}}{p_{\mathrm{ic}}}$
r_c	Compression ratio of the engine
R_{c}	Specific in cylinder gas constant at intake valve closing
R_{im}	Specific gas constant in the intake manifold
T_1	Temperature of charge (air, fuel, and residual gases) at start of compression
T_{af}	Temperature of air/fuel charge
T_{ic}	Air temperature between intercooler and throttle
T_{im}	Intake manifold temperature
T_r	Temperature of residual gases
t_0	Time in seconds for the injector needle lift

continued from previous page	
Symbol	**Description**
t_{inj}	Time in seconds where the injector is open
V_c	Clearance volume
V_d	Displacement volume
V_{im}	Volume of intake manifold
V_r	Volume of residual gases
W_{a}	Measured air-mass-flow
W_{at}	Air-mass-flow through throttle
W_{c}	Air-mass-flow to cylinder
$W_{\text{c}_{\text{std}}}$	Air mass flow to cylinder using mapped volumetric efficiency
$W_{\text{c}_{\text{ts}}}$	Air mass flow to cylinder using mapped volumetric efficiency with estimated offset $\Delta\eta_{\text{vol}}$
x_r	Residual gas fraction
y_L	Fraction of untreated emissions that leaks out
α	Throttle angle
γ	Ratio of specific heats $\frac{c_p}{c_v}$
η_i	Conversion efficiency of the TWC for specie i
η_{vol}	Volumetric efficiency
$\Delta\eta_{\text{vol}}$	Offset in volumetric efficiency
$\Delta\hat{\eta}_{\text{vol}}$	Estimated offset in volumetric efficiency
λ	Normalized air/fuel ratio $\frac{m_a}{m_f\left(\frac{A}{F}\right)_s}$
λ_{est}	Estimated normalized air/fuel ratio
$\overline{\lambda_{\text{est}}}$	Mean value of estimated normalized air/fuel ratio
μ_x	A general test statistic
σ_v	Standard deviaion of noise